



Strength prediction of circular CFST columns through advanced machine learning methods



Chao Hou ^{a,b,*}, Xiao-Guang Zhou ^a

^a Department of Ocean Science and Engineering, Southern University of Science and Technology, Shenzhen, 518055, PR China

^b Southern Marine Science and Engineering Guangdong Laboratory (Guangzhou), Guangzhou, 511485, PR China

ARTICLE INFO

Keywords:

Concrete-filled steel tube (CFST)
Machine learning (ML)
Strength prediction
Axial compression strength
Correlation analysis

ABSTRACT

Concrete-filled steel tube (CFST), well recognized for its excellent mechanical behaviour and economic efficiency, is widely used as a main load-carrying component in various kinds of structures. Machine learning (ML) is one of the promising artificial intelligence methods which just starts to be utilized for the advanced prediction of structural performances. This paper attempts to evaluate the feasibility of combining mechanism analysis to optimize ML models in predicting the axial compression strength of circular CFST columns. A comprehensive database containing 2,045 circular CFSTs under axial loading was established through extensive literature survey. Based on correlation analysis and mechanism analysis, input parameters for ML models were rationally selected. Then back-propagation neural network (BPNN), genetic algorithm (GA)-BPNN, radial basis function neural network (RBFNN), Gaussian process regression (GPR) and multiple linear regression (MLR) models were established. It was revealed that the established ML models, especially GPR, could reliably predict the strengths of CFST with higher accuracies and wider applicable ranges than existing methods in current design standards. By subdividing the database according to column slenderness, ML models achieved improved accuracy for strength prediction, whilst little effect on the model accuracy was generated by random subdivisions. This indicates that when adopting ML methods in structural engineering sector, optimization of the models can be expected on the basis of rational understanding towards the corresponding structural mechanism.

1. Introduction

Machine Learning (ML), as a method to realize artificial intelligence (AI), is to explore hidden laws from existing data for prediction or classification [1]. In other words, ML constructs the mapping relationship between data inputs and outputs, so as to replace the functions between them which would otherwise be too complicated to express explicitly. Nowadays, ML method is increasingly applied in many aspects of structural engineering, most of which are predictions on material properties, such as strength [2–4] and elastic modulus [5,6], while predictions on the performance of structural members are relatively limited [7–12]. Currently, experiment and finite element method (FEM) are still two mainstream ways to predict member performances. Although physical experimentation provides valuable data and observations, the resource consumption and waste emission of repeated tests are considerable. As can be expected, using ML to predict member performances not only provides references for practical design, but also makes the best of completed experimental data to reduce the demand of further tests and thus save vast resources. Due to the complex material

* Corresponding author. Department of Ocean Science and Engineering, Southern University of Science and Technology, Shenzhen, 518055, PR China.
E-mail address: houc@sustech.edu.cn (C. Hou).

Nomenclature

A	Sectional area of CFST ($=A_s + A_c$)
A_c	Sectional area of concrete
A_s	Sectional area of steel
B	Sectional width of square/rectangular CFST
D	Sectional diameter of circular CFST
E_c	Elastic modulus of concrete
E_s	Elastic modulus of steel
f_c	Prism compressive strength of concrete
f'_c	Cylinder compressive strength of concrete
f_{cu}	Cube compressive strength of concrete
$f_{cu,150}$	Cube compressive strength of concrete tested by 150 mm width cube
f_y	Yield strength of steel
H	Sectional height of square/rectangular CFST
L	Length of CFST column
N_{ue}	Measured axial compression strength of CFST from tests
t	Thickness of the steel tube
α	Sectional steel ratio ($=A_s/A_c$)
ξ	Confinement factor of CFST [$=(f_y A_s)/(f_c A_c)$]
λ	Slenderness ratio ($=4 L/D$ for circular CFST; $= 2\sqrt{3}L/B$ for square/rectangular CFST)
φ	Stability factor of a column under axial compression

properties, contact relationships, boundary conditions, etc., the results of FEM are greatly influenced by the technical skills of the modeler. However, ML operates based on laws between a large amount of experimental data, which is much less dependent on the user itself [13]. Therefore, it is worthwhile attempting to use ML methods for predicting strengths of structural members, so as to provide a basis for further predictions of structural connections and complex structural systems. The well-known and widely-utilized structural member, concrete-filled steel tube (CFST), appears befitting to evaluate the feasibility of ML methods, given that its strength calculation is quite complicated due to the multiple effects of geometries, material properties, and nonlinear passive material interactions. Meanwhile, a large amount of existing test data on CFST columns also facilitates the application of ML methods.

As is known, CFST is a kind of structural member formed by filling concrete into a steel tube, as shown in Fig. 1(a). When subjected to axial compression, the concrete infill can delay or avoid the buckling of steel tube, while the confinement provided by steel tube effectively improves the mechanical properties of concrete. A circular steel tube can provide more uniform confinement on the

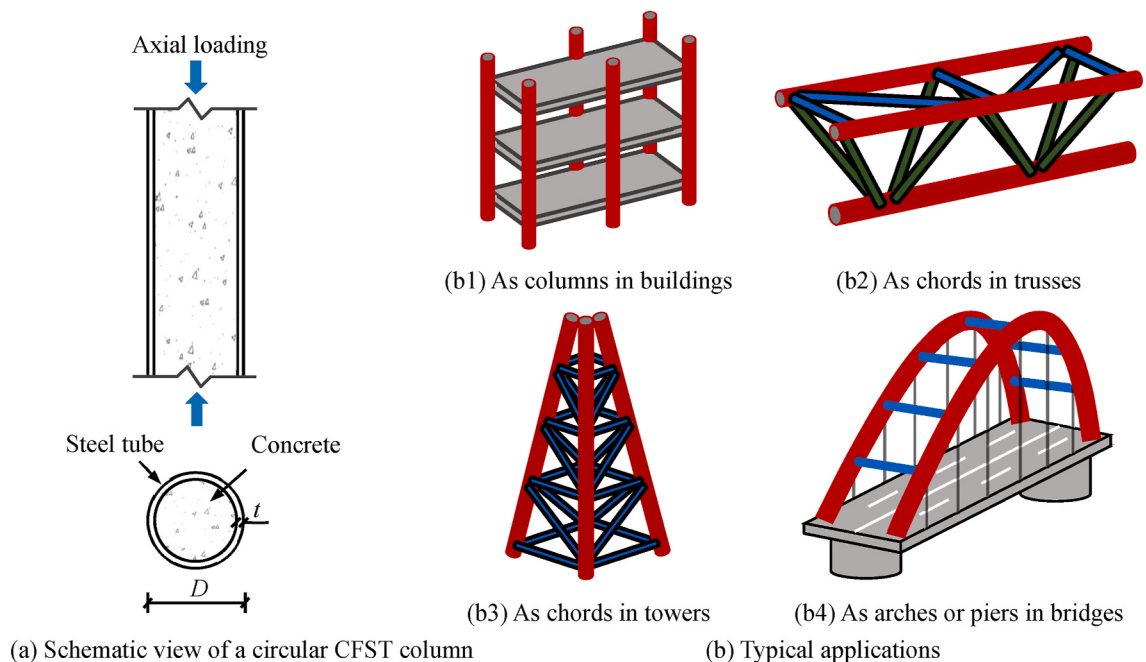


Fig. 1. Sketch of a circular CFST column and its typical applications in practice.

concrete than a rectangular one, resulting in relatively higher strength and ductility for circular CFST columns [14–17]. Therefore, applications of circular CFST columns in buildings, bridges, towers, trusses, and other types of structures have become increasingly popular in the past few decades [18,19], as illustrated in Fig. 1(b).

Furthermore, there exists a practical demand for predicting the axial compression strength of CFST using ML methods. Although the strength can be calculated by many existing design standards [20–25], which have respective applicable ranges as listed in Table 1, where f_c , f_c' , and f_{cu} are respectively the prism, the cylinder, and the cube compressive strength of concrete; D is the sectional diameter of CFST; f_y , E_s , and t are respectively the yield strength, the elastic modulus, and the thickness of steel tube. Nowadays, high-strength steel, high-strength concrete, and large-sized mega CFSTs are increasingly applied in practice. The material strength, geometric dimension and section slenderness of the actual columns may far exceed the applicable ranges of the above mentioned standards, indicating potential risks to calculate their strengths using these standards. In recent years, many scholars have conducted experimental studies on high-strength or large-scale CFST columns [26–28], from which a database covering a wider range of parameters can be established. This facilitates ML methods for overcoming the limited applicable ranges of existing design standards.

ML methods were applied earlier in predicting the strength of rectangular CFST columns. In 2004, Hao and Zhai [29] established a three-layer back-propagation neural network (BPNN) to evaluate the strength of 50 rectangular CFST stub columns subjected to axial compression, and concluded that a better model can be obtained by supplementing training data. Gao et al. [30] and Zhu et al. [31] conducted similar studies, with databases containing 66 and 55 samples, respectively. As can be seen, early researches initiated ideas for applying ML methods in CFSTs, but the sizes of databases were relatively small, resulting in limited applicable ranges of the obtained models. The applicable range of BPNN established by Zarringol et al. [11] was greatly extended, since 895 samples in their database covered a wide range of material strength, geometry, and slenderness. In addition, BPNN has also been used to study the eccentric compressive strength of rectangular CFSTs [11,32,33].

Comparatively, available research is limited on ML methods for predicting the strength of circular CFST columns under axial loading. The features of previously established databases and ML models are summarized in Table 2. Kheyroddin et al. [34] used BPNN to predict strengths of CFSTs, and the average error of predictions was 5.76%, indicating a good accuracy. A BPNN model was developed by Tran et al. [35] for predicting the axial strength of CFSTs with ultra-high-strength concrete ($100 \leq f_c' \leq 200$ MPa), however, their database were obtained by FEM rather than actual tests. Vu et al. [12] used gradient tree boosting (GTB) algorithm to predict the strengths of 1,017 CFSTs, and found that GTB had superior accuracy than standards and empirical formulas. Using ML methods to predict axial compressive strength and seismic performance of circular recycled aggregate CFST columns has also been reported [36,37].

It should be noted that most of the previous research directly apply ML methods for the prediction of CFST columns, whilst optimization algorithm is rarely used to improve the performance of ML models in strength predictions. Nguyen et al. [41] used invasive weed optimization (IWO) algorithm to adjust and optimize weights and biases of feedforward neural network (FNN), where the outcomes showed that using IWO to optimize FNN can effectively improve the accuracy, with R^2 increased from 0.919 to 0.979. Additionally, limited research has been conducted on the selection of input parameters of ML models for CFSTs besides the application of grey relational analysis (GRA) in Ref. [37]. The input parameters of ML models for CFSTs include basic parameters, such as D , t , L , f_y , and f_c' ; and secondary parameters, such as H/B , D/t , H/t , B/t , steel ratio (α), confinement factor (ξ), and slenderness ratio (λ) [29,31,42,43]. Du et al. [42] used BPNN to predict the axial strength of 305 rectangular CFSTs and found that adding five secondary parameters (H/B , H/t , B/t , α , ξ) would reduce the model accuracy, whilst Zhang et al. [43] conducted a similar research and reached an adverse conclusion. This certifies a demand for in-depth investigation on the selection of suitable inputs for ML methods. It is worth mentioning that the formulas in existing literatures and standards are based on numerous mechanical analysis, which can provide a basis for scientifically selecting the inputs of the established ML methods.

In summary, ML provides an innovative method for predicting the strength of a CFST column. Although there exists some previous researches with proposed simplified formulas [10,11,35,37], more work is needed especially for the following reasons:

- (1) The strength of CFST is affected by many parameters, whilst most researchers select them as inputs without clarifying the mechanical principles explicitly. In order to improve the physical significances of the established ML model, it is necessary to scientifically select input parameters for ML models through the combination of mechanics and correlation analysis.
- (2) The number and type of samples in the database impose a remarkable impact on the applicability and accuracy of ML models. Through extensive literature review, the number of tested samples and the corresponding parameter ranges can be further supplemented to establish a comprehensive test database.

Table 1
Applicable ranges of existing design standards for circular CFST columns.

	ACI 318 (2014) [20]	EC 4 (2004) [21]	AISC 360 (2016) [22]	AS/NZS 2327 (2017) [23]	GB/T 51446 (2021) [24]	GB 50936 (2014) [25]
f_y (MPa)	–	235–460	≤ 525	≤ 690	235–460	235–420
f_c'/f_{cu} (MPa)	$f_c' \geq 17.2$	$20 \leq f_c' \leq 50$ $25 \leq f_{cu} \leq 60$	$21 \leq f_c' \leq 69$ for normal concrete $21 \leq f_c' \leq 41$ for lightweight concrete	$f_c' \leq 100$	$f_{cu} \geq 30$	$30 \leq f_{cu} \leq 80$
D/t	$\leq \sqrt{8E_s/f_y}$	$\leq 90 \frac{235}{f_y}$	$\leq \frac{0.31E_s}{f_y}$	$\leq \frac{0.31E_s}{f_y} \times \frac{250}{f_y}$	$\leq 150 \frac{235}{f_y}$	$\leq 135 \frac{235}{f_y}$

Table 2

Summary of machine learning model studies on circular CFST columns subjected to axial compression.

Reference	Features of the established database						Features of the adopted machine learning model		
	Number of test samples	D (mm)	t (mm)	L (mm)	f_y (MPa)	f_c' (MPa)	Algorithm	Topology	Input parameters
Kheyroddin et al., 2013 [34]	150	—	—	—	—	—	BPNN	5-9-1	Basic parameters
Ahmadi et al., 2014 [38]	272	82.5–179	0.7–12	200–500	200.2–853	17.40–106.02	BPNN	5-9-1	
Güneyisi et al., 2016 [39]	314	60–1020	0.70–13.25	152.3–3060	15–130.18	185.7–853	GEP	N/A	
Nour and Güneyisi 2019 [36]	97	88–219	1.65–4.66	285–657	176.5–465	22.6–52.9	GEP	N/A	
Tran et al., 2020 [35]	768	300–600	6–30	900–4800	235–460	100–200	BPNN	6-11-1	
Zarringol et al., 2020 [11]	1305	45–1020	0.52–16.54	153–5560	179–853	8–185	BPNN	5-5-5-1	
Naser et al., 2021 [40]	1245	44.45–1020.00	0.52–16.54	152.35–5560.00	178.28–853.00	9.17–193.30	GA; GEP	N/A	
Vu et al., 2021 [12]	1017	44.5–1020	0.52–16.54	152.35–5560	178.28–853	7.59–185.94	GTB; RF; SVM; DT; DL	N/A	
The current study	2045	38.1–1020	0.52–16.72	152.35–5560	176.5–1233	10–186	BPNN; GA-BPNN; RBFNN; GPR; MLR	5–12–1	Basic/secondary parameters

Notes: 'BPNN' stands for the back-propagation neural network; 'RF' stands for the random forest; 'SVM' stands for the support vector machine; 'DT' stands for the decision tree; 'DL' stands for the deep learning; 'GEP' stands for the gene expression programming; 'GA' stands for the genetic algorithm.

(3) In existing studies, researchers tended to use the global database as a whole for training/testing ML model. However, the huge differences in failure mechanisms between long and stub CFST columns may affect the laws between inputs and strengths. Potential risks need to be testified.

(4) Most studies focused on using BPNN to predict the axial compression strength of CFST columns, as listed in [Table 2](#), whilst other supervised ML algorithms such as radial basis function neural network (RBFNN) and Gaussian process regression (GPR) are rarely applied. In addition, optimization algorithms may be attempted to optimize ML model for better performance, yet research in this aspect is limited.

This paper attempts to optimize ML models through the implementation of mechanism analysis to improve their physical significance and prediction efficiency, so as to reliably predict the axial compression strength of circular CFST columns. The overall framework of this research is illustrated in [Fig. 2](#). Firstly, a comprehensive database composed of 2,045 circular CFSTs under axial compression is established. Secondly, input parameters of ML model are selected scientifically combined with mechanism analysis and correlation analysis. Then BPNN, genetic algorithm (GA)-BPNN, RBFNN, GPR as well as multiple linear regression (MLR) models are established and compared. Finally, the influence of database subdivision methods on the model accuracy, such as random subdivision and conditional subdivision, is rationally evaluated.

2. Database of circular CFST columns under axial compression

2.1. Selection criteria of the test data

In order to ensure the suitability and consistency of the test database on circular CFST columns, the following criteria are applied when establishing the experimental database:

- 1) Circular CFST columns tested under monotonic axial loading are selected, where the entire cross-sections, i.e., both concrete and steel tube, need to be fully loaded. There is no limitation on the sectional dimensions or the column lengths in order to collect extensive test data.
- 2) Considering that different types of concrete may affect the failure mechanisms of CFSTs, only normal and high-strength concrete are collected, whilst recycled aggregate concrete, steel fiber concrete, rubber concrete, expansive concrete, etc. are excluded. There is no limitation on the compressive strengths of concrete.
- 3) Only low carbon steel tube is selected, whilst stainless steel tube and aluminum tube are excluded. There is no limitation on the yield strengths of steel.
- 4) Strengthened CFST columns by internal reinforcements, stiffeners or external wrapping such as fiber reinforced polymer (FRP) are not included in the database. CFST columns experiencing high temperature or freeze-thaw cycles are not included either.
- 5) At least the six main basic parameters of the tested CFST columns need to be reported in references, i.e., D , t , L , f_y , f_{cu} (or f'_c or f_c) and N_{ue} . In some literatures, these basic test parameters were not fully provided, and the corresponding specimens were therefore excluded in the database.

2.2. Conversion of the concrete strength

The established database covers test data obtained by researchers from worldwide, where various concrete compressive strength measurements are adopted in different testing programs, including cylindrical tests, cubic tests, and prismatic tests with different sample dimensions. The strengths of concrete need to be converted so as to facilitate the processing of ML methods. In the current study, all concrete strengths are converted into the compressive strength of 150 mm width cube ($f_{cu,150}$). This is mainly due to the fact that cube strengths are adopted in most references. The following strength conversion methods are adopted.

i) Shape conversion

The shape conversion method proposed by the Code for Design of Concrete Structures in China (GB 50010) [44] and Goode and Lam [45] are used.

$$f_c = \alpha_1 \alpha_2 f_{cu} \quad (1)$$

$$f'_c = 0.8 f_{cu} \quad (2)$$

where f_c , f_{cu} , and f'_c respectively indicate the prism, the cube, and the cylinder compressive strength of concrete; α_1 and α_2 are shape conversion factors, which can be determined by Ref. [44].

ii) Size conversion

The strength measured from non-standard specimen should be multiplied by the size conversion factor, which can be found in the Standard for Test Methods of Concrete Physical and Mechanical Properties (GB/T 50081) [46]. Taking the non-standard cube specimen with $100 \times 100 \times 100$ mm as an example, its strength needs to be multiplied by a size conversion factor of 0.95 to reflect the strength of a standard specimen ($150 \times 150 \times 150$ mm).

2.3. Description of the established database

Following the selection criteria described in Section [2.1](#), an extensive database consisting of 2,045 tested circular CFST columns

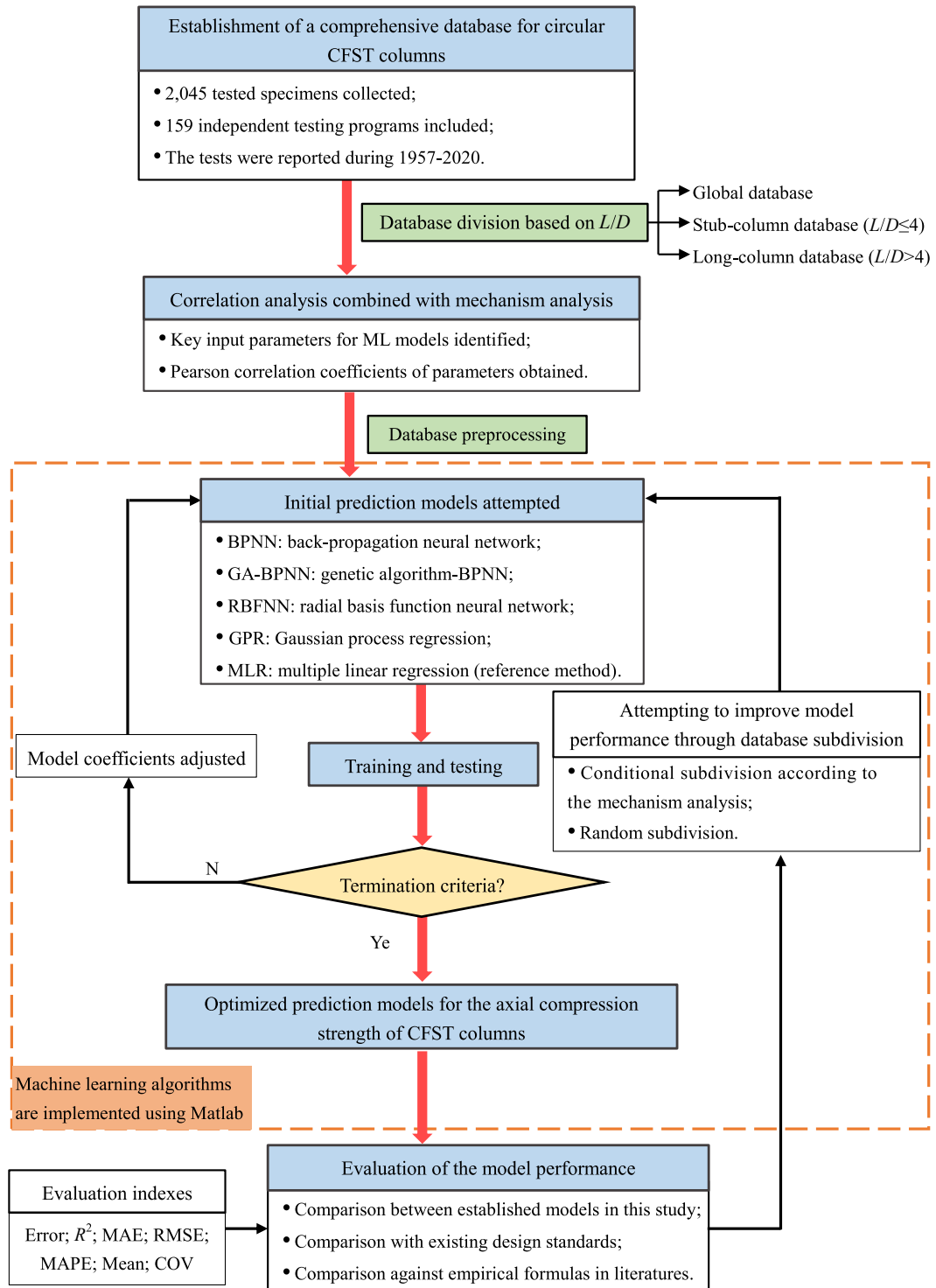


Fig. 2. Flow chart for axial compression strength prediction of CFST using machine learning models.

under axial compression is established in this study, accounting for approximately 91% of the gross collected samples. Among them, 1,311 test samples are from Refs. [15,19,27,28,47–154] and the remaining 734 samples are from Goode's open database [45] (364 samples are from the original references [26,155–171], and the rest 370 are directly from Goode's database [45] since the authors cannot access the original references). These CFST column tests are from 159 independent experimental programs conducted during the years 1957–2020 by researchers worldwide. Detailed information of the data sources in the database is summarized in Table 3.

Table 3

Information of the database sources collected in this study.

No	D (mm)	t (mm)	L (mm)	f_y (MPa)	f_{cu} (MPa)	Number	Ref.	No	D (mm)	t (mm)	L (mm)	f_y (MPa)	f_{cu} (MPa)	Number	Ref.
1	108–450	2.96–6.47	324–1350	279–853	30.16–101.06	36	[47]	66	129–133	3.0–5	387–399	306	53.7–69.7	9	[109]
2	140–141.4	3–6.68	605.4–616	285–537	29.76–35.23	3	[15]	67	160	3.46	480	363	78	1	[110]
3	200–300	2.0–5	600–900	265.8–341.7	33.94–38.94	3	[48]	68	108	4	324–1944	336	54.9	3	[111]
4	159–164	3.8–6.3	520	342–379	40.15	12	[49]	69	193.7	8	3315	444	50–177.5	2	[112]
5	111.3–250	1.65–9	337–750	248–433	46.48–81.86	13	[50]	70	165.2	3.7	495.6	366–372.6	35.03–96.9	5	[113]
6	159.6–160.3	4.96–5.2	200–4000	270–283	50.00–132.50	18	[51]	71	230	2.3	690	360.8	38–76	2	[114]
7	165–190	0.86–2.82	577.5–664.5	185.7–363.3	48.69–128.25	15	[52]	72	88.8–133.4	2.98–3.98	266.5–399	980–1233	44.38–143.63	13	[115]
8	219	7	990–1640	273	55.82	12	[53]	73	140	2	500	413	35.2–54.8	3	[116]
9	108	4	3510–4158	348.1	31.8–46.8	11	[54]	74	90	1.9	270	359	37.2–56.1	6	[117]
10	114.3–267.4	3.1–6.4	661–4956	340–505	48.57–74.93	37	[55]	75	90	1.92	270	359	37.2–36.1	6	[118]
11	110–165	1.9–4.7	2200–2475	350–355	33.4	6	[56]	76	165	2.37	615	287.5	30.2	2	[119]
12	60–180	1.48	180–1500	307	42.6	4	[57]	77	273	7	822	385	70.2	3	[120]
13	152	1.65	500–900	270–328	91.25–106.25	6	[58]	78	108	4.5	700–3470	400	69	10	[121]
14	108–133	4.5–4.7	378–1620	352–358	100.7–110.2	12	[59]	79	152–219	4.5–10	480–657	280–377	75–85.5	10	[122]
15	111.3–160	2–2.5	750	250	34.49	2	[60]	80	120	2.65	360–1400	340	20.1–36	3	[123]
16	60–250	1.87–2	180–750	282–404	85.2–90	26	[61]	81	114	3.0–4	350	360–383	51–109	63	[124]
17	159	4.8–10	650	355–433	52.3–117.2	9	[62]	82	108	4	324	336	54.9	1	[125]
18	220	4	1000	366	42.08	1	[63]	83	219	4.0–7	657–1314	326–338	29.24	18	[126]
19	133.1–167.8	3.28–5.44	396–504	325.3–392	42.37–73.25	36	[64]	84	38.1–216	0.55–12.8	247.8–2590.8	264.89–605.44	17.08–50.52	106	[127]
20	133.1–138.5	3.24–5	339.15–415.5	331.7–351	83.73	2	[65]	85	150–165	1.2–1.6	1200	375	32.9–34.9	3	[128]
21	114.3	3.05	320	380	48.69	1	[66]	86	219	4.0–6	1000	325	47.6–58	3	[129]
22	114.3–219.1	3.6–10	250–600	300–428	61.28–219.81	12	[27]	87	159	4.8	650	433	79.4	1	[130]
23	219.1–273	10.0–16	3810	374–412	213.75–220.88	2	[67]	88	76	2	1555	275	52	1	[131]
24	100–200	1.98–3.82	300–600	388–432	65.8	10	[68]	89	250–500	5.0–10	750–1500	333–342	38	4	[132]
25	140–323.9	0.95–16.72	420–1000	184.8–1153	62.5–146	26	[19]	90	96–273	5.0–8	450–1100	274–410	43.38–45.63	3	[133]
26	121–152	5–8.5	370–465	275–295	111.8–137.3	14	[69]	91	198.9–200.3	1.99–2.98	398–401	397–408	56	3	[134]
27	557.8–559.5	16.53–16.54	1115.6–1119.1	546	31.7	3	[70]	92	165	3.0–4	500	338	100.64	6	[135]
28	114.3	2.74–5.9	300–900	235–355	66.74–127.3	18	[71]	93	90	1.78–1.9	270	210–264	37.2	4	[136]
29	114.3	3.35–6	342.9–1143	287.33–342.95	26.72–125.28	36	[72]	94	89	2.0–4	300	257–269	26.5–45.3	9	[137]
30	133–219	4.5–6.3	708–3078	300–405	42.2–135	7	[73]	95	133	3.0–12	400	290–376	152.79–215.87	22	[138]
31	165–219	2.72–4.78	510–650	350	42.6–77.2	6	[74]	96	125–133	1.0–5	400–465	244.9–319.3	147.63–158.75	18	[139]
32	108–133	1.0–7	378–465	232–429	51.3–110.2	20	[75]	97	102–152	4.0–6	450	291.4–321.6	81.13–107.92	6	[140]

(continued on next page)

Table 3 (continued)

No	D (mm)	t (mm)	L (mm)	f_y (MPa)	f_{cu} (MPa)	Number	Ref.	No	D (mm)	t (mm)	L (mm)	f_y (MPa)	f_{cu} (MPa)	Number	Ref.
33	127–203	4.2–9.6	480–800	349–427	115.4	9	[76]	98	83–133	4.0–12	400–996	294–453	113.19	17	[141]
34	153–477	1.54–11.36	306–954	290–345	85.4	36	[77]	99	110–113	5–6.5	300	310–321	127.21–154.85	5	[142]
35	215.9–632.1	2.6–11.2	657–1890	259.8–590.4	59.78	12	[78]	100	133	6.0–10	466–1596	352–376	142.12	16	[143]
36	88–110	2.7–3	303–404	398–410	61.45–72.14	5	[79]	101	152–159	4.5	3000	344.4–475.4	33.75–108.88	16	[144]
37	182.48–346.49	1.99–4.69	548–1039	311.6–362.5	67.88	18	[80]	102	164.97	2.92	595	389.3	61.4	2	[28]
38	114–167	3.1–5.6	250–350	300	53–70	6	[81]	103	150–401	3.2	620–1680	265	30.16	9	[145]
39	101.3–318.5	3.02–10.38	303.9–955.5	335–452	27.55–61.99	13	[82]	104	200	6	695	451	47–121.1	7	[146]
40	149–165	1–8.0	500	338–438	82.75–87.21	26	[83]	105	140–216.3	4.5–8.2	420–648.9	371.9–462.9	33.25–61.75	18	[147]
41	76.43–152.7	1.68–4.93	152.35–1676.4	363.03–632.98	26.1–54.26	24	[84]	106	164.1–189.2	1.5–5.7	636–735	363–452	194.63–220.25	6	[148]
42	150–273	3–4.5	465–704	318.3–380	38.3–60.5	21	[85]	107	168–219	6	672–876	496.4	30–50	6	[149]
43	209–211	2.0–3	1370–2170	256–297	34.38–44.5	5	[86]	108	128	4	400	248	44.9	1	[150]
44	140.84–262	2.11–3.04	525–975	691–734	50.4–53.4	15	[87]	109	131.8–133.9	3.2–5.8	350	320–345	44.2	4	[151]
45	300	4.5–11.88	900	347.9–471.38	32.93–97.87	12	[88]	110	218.9–600	2.95–5.99	530–1200	280–326	15.05	12	[152]
46	219	3.0–5	700	313	62.5	3	[89]	111	146–154	3.0–7	350	593.2–594.5	34.6–54.3	6	[153]
47	89.2–1020	0.95–13.25	248–3060	249–476.2	18.75–156.63	49	[90]	112	114–168	4.5–16	342–504	285–320	95	14	[154]
48	101.6–139.8	2.37–3	304.8–419.4	341.04–462.56	24.11–128.85	29	[91]	113	95–500	1.5–12	240–5000	191.79–602.7	26.75–68.43	105	[155]
49	127–133	1.5–4.5	400	310–350	54.74	4	[92]	114	92–300	1.5–10	202–1994	232.26–631.12	26.75–95.39	76	[156]
50	202–204	1.0–2	400	226–242	44.88–52.75	3	[93]	115	96–320	2.0–12	200–1100	235.2–410.62	32.93–55.57	43	[157]
51	180	3.8	740	360	64.1	2	[94]	116	166	5	710–3700	277.34–313.6	34.68–51.24	10	[158]
52	102	2.94	702	320	61.7–74.2	4	[95]	117	108	4	324–5560	338.88	35.71	26	[159]
53	165	3.54	480	368	50.5	1	[96]	118	169	7.5	690–1768	360	88.47	3	[160]
54	90	1–1.5	300	328.95	36.4	9	[97]	119	108–133	1.0–7	378–465	232–429	100.7–110.2	16	[161]
55	114	1.42–2.78	500–1000	331.8–387.2	12.2	5	[98]	120	101.3–318.5	3.03–10.37	305–955	335–452	27.55–61.99	13	[162]
56	100–180	1.2–2	369–620	216–253.3	20.53–49.26	14	[99]	121	108	4.5	3510–4158	348.1	30.21–44.46	11	[26]
57	500	7	2000	365	71.59–79.73	3	[100]	122	114.29–115.04	3.75–5.02	300–300.5	343–365	31.4–104.9	8	[163]
58	90	1–1.5	300	328.95	36.4	9	[101]	123	100–200	3	300–600	303.5	58.5	4	[164]
59	320–400	1.51–2.71	960–1200	294–359.1	28.5–31.92	18	[102]	124	150	0.7–2.1	480–800	247.53–248.2	28.18–44.1	6	[165]
60	219	4.8	740	260	44.4–47.9	9	[103]	125	100	1.9	300–3000	404	121.6	10	[166]
61	139	0.92–1.92	500–1200	293–427.66	41.21	9	[104]	126	300–360	6.0–12	900–1080	479–498	39.38	2	[167]
62	114.3–219	2.34–3.9	456–1980	315–373	66–80	22	[105]	127	114.85–193.7	3–3.5	1000–2500	345.2–488.2	29.36–38.29	24	[168]
63	127–136	1.5–6	381–408	330	54	5	[106]	128	150	3	675–900	324.4	59.3	2	[169]
64	100	2–3.9	300	176.5–235.1	83.9	3	[107]	129	111.64–113.64	1.9–3.64	400	259.6–261.3	47.8–56.7	3	[170]
65	508	8.76	1500	360.4	70.91	1	[108]	130	159	6	2135	394–487	47.13–145	2	[171]

As mentioned in the Introduction session, researchers generally used the global database to train ML model. Considering the differences of failure mechanisms between long and stub CFST columns, CFST columns are categorized as stub columns ($L/D \leq 4$) and long columns ($L/D > 4$), according to technical code GB 50936 [25]. The global database (GD) are therefore divided into two groups: i) Stub-column database (SCD) contains 1,259 samples, accounting for 61.56% of GD; ii) Long-column database (LCD) includes 786 samples, accounting for 38.44% of GD. In the following sections, the three databases are used respectively to construct ML models in order to evaluate the impact of database subdivision on the model accuracy.

2.4. Statistical properties of the global database

Fig. 3 illustrates statistical distributions of CFST samples in the established global database. It can be observed that basic and secondary parameters approximately show normal distribution patterns. Various types of CFST columns are included in the global database. More specifically,

- The database includes small-sized CFSTs with diameter as small as 38.1 mm and full-scale CFSTs with diameter up to 1,020 mm.
- The thickness of steel tube varies from 0.52 mm to 16.72 mm with an average of 4.43 mm.
- The lengths of CFSTs are mostly distributed between 200 mm and 1,200 mm, while stub columns with length as short as 152.35 mm and long columns with length as long as 5,560 mm are also included.
- The ranges of material strengths vary from normal to ultra-high strengths, with the concrete strength up to 220.88 MPa and the steel strength as high as 1,233 MPa.
- As for the secondary parameters, L/D of columns ranges from 0.81 to 51.48; D/t of CFST sections varies from 7.13 to 264.90. This means that stub and slender columns as well as compact, non-compact, and slender sections are all included in the database. The confinement factor ξ and steel ratio α are also distributed widely, being 0.04–12.90 and 0.015–0.93, respectively.

It should be noted that above ranges of key parameters have far exceeded the applicable ranges of existing standards, as mentioned in the previous sections. Therefore, the established database facilitates ML methods for an extended range of CFST strength predictions.

2.5. Limitations of the established database

Due to the extensive sources of data covered in the database and some inevitable simplified assumptions when establishing it, the database has the following limitations.

- In some of the literatures, the dimensions of samples for concrete compressive strength tests were not provided, yet the sample types (cube, cylinder or prism) were demonstrated. In this case, standard sample dimensions, namely $150 \times 150 \times 150$ mm cube, $\varphi 150 \times 300$ mm cylinder, or $150 \times 150 \times 300$ mm prism, are assumed.
- The actual lengths of the CFST column specimens reported in the literatures are used, while the thicknesses of potential loading plates or spherical hinges are excluded.

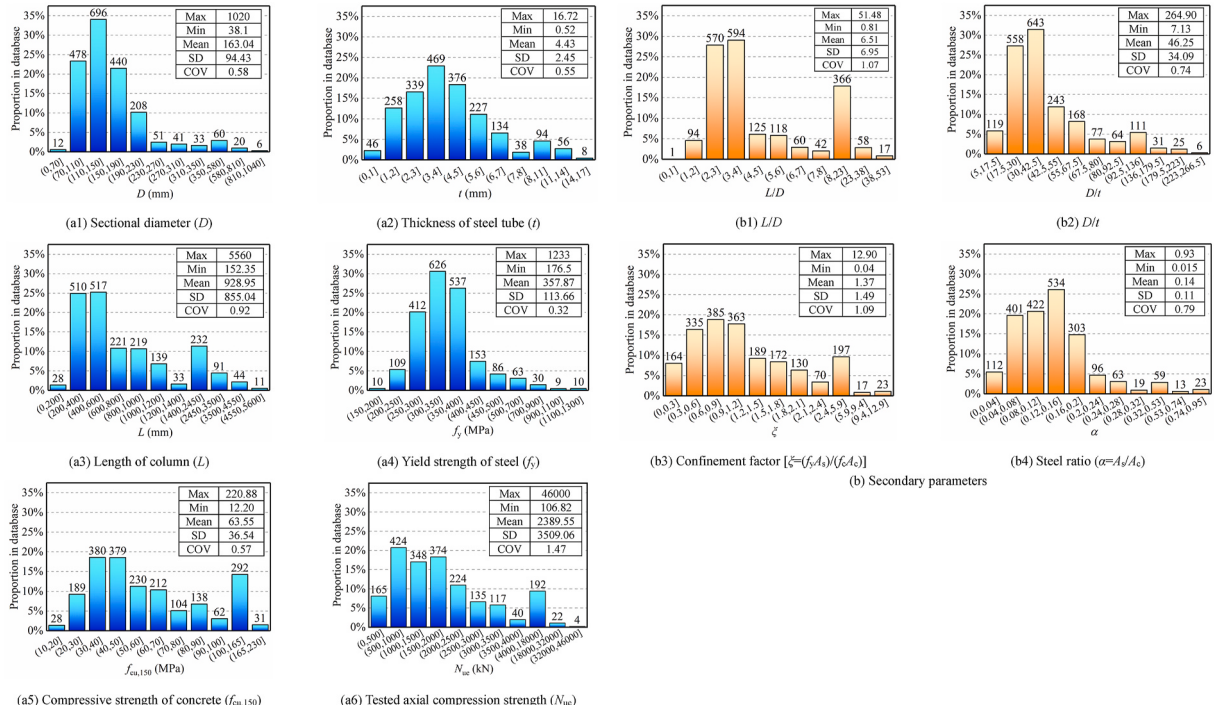


Fig. 3. Statistical distributions of the CFST samples in the established global database.

- Since the collected experiments were conducted in different ages and regions, the potential systematic differences in terms of testing rigs, loading speeds, measurement accuracies, etc., were not considered in the database. However, since the axial compression strength is the main focus here, the influence of the above factors is believed to be mild.

3. Identification of key parameters through correlation analysis

It can be concluded from previous studies that the strengths of CFST columns are affected by many factors, which can be divided into basic parameters, such as dimensional factors D , t , L as well as material factors f_y , f_{cu} / f_c / f'_c ; and secondary parameters, such as sectional area of steel (A_s), sectional area of concrete (A_c), sectional area of CFST ($A = A_s + A_c$), $f_y A_s$, $f_{cu} A_c$, L/D , etc. [14,19–25,51,70] As mentioned above, limited research has been conducted on the selection of input parameters of ML models. Only Xu et al. [37] applied GRA to select input parameters, and Nguyen et al. [41] investigated the correlation between different parameters. However, limited parameters (basic parameters only) were investigated in existing research on circular CFSTs, while mechanical principles were seldomly considered when selecting the input parameters. This demonstrates a need for in-depth investigation on the method of selecting suitable input parameters for ML models, where the parameters utilized in existing standards [20–25] can provide valuable references.

On the other hand, failure mechanisms between long and stub CFST columns are quite different. A long column usually exhibits large lateral deflection and fails due to the loss of stability. However, a stub column mainly shows sectional failure without obvious overall buckling [14,71,115]. The difference in failure mechanism may change the influence of parameters on the column strength. From this point of view, it is to an extent unreasonable to analyze the global database directly. Therefore, correlation analysis is conducted to analyze three databases (global database, stub-column database, and long-column database) separately, where the correlation between two kinds of parameters and strength is evaluated. Correlation analysis is a statistical method, which can quantitatively measure the correlation between two variables [172]. The Pearson correlation coefficient is defined as:

$$r = \frac{n \sum_{i=1}^n x_i y_i - \sum_{i=1}^n x_i \sum_{i=1}^n y_i}{\sqrt{n \sum_{i=1}^n x_i^2 - (\sum_{i=1}^n x_i)^2} \sqrt{n \sum_{i=1}^n y_i^2 - (\sum_{i=1}^n y_i)^2}} \quad (3)$$

where x_i and y_i represent two parameters, and n is the total number of samples. When r is closer to 1, a strong positive correlation is indicated; when r is closer to 0, a weak correlation is represented; when r is closer to -1 , a strong negative correlation is reflected.

Table 4 lists the concrete information in literatures and the corresponding r with CFST strength. It can be found that f_{cu} reported in references accounts for the highest proportion (66.27%), and r between f_{cu} and CFST strength is slightly higher than the other two types of concrete strength. In order to predict the strength of CFST columns conveniently and reduce the errors caused by strength conversion, only f_{cu} is used in the following sections.

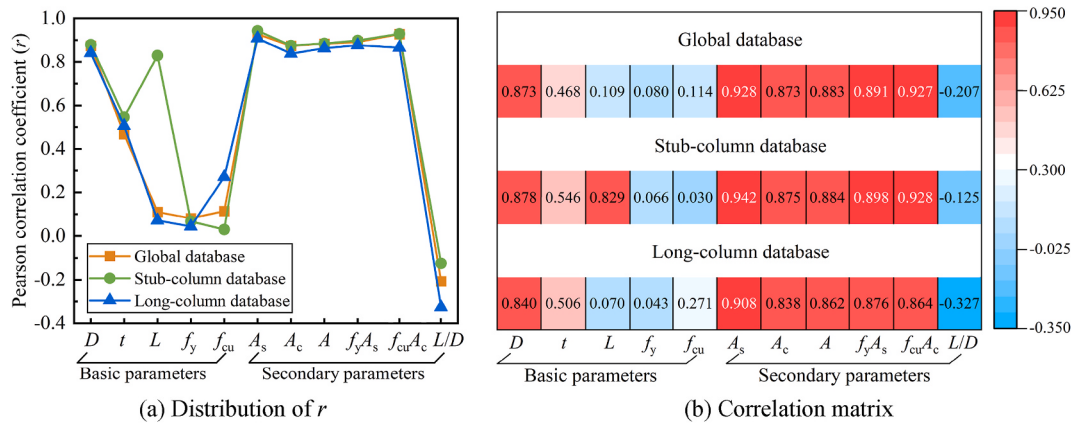
Correlation analysis is then carried out to identify parameters that have significant influence on the strength of CFST, with the results presented in **Fig. 4**. Combined with mechanism analysis, the following findings can be reached:

- For each database, the sectional dimension of CFST columns, involving D , t , A , A_s , and A_c , exhibits a strong correlation with the column strength, which is consistent with theoretical senses and conclusions in previous references [10,12]. These parameters are generally used in standards and references [11,20–25,173] to reflect the impact of sectional dimensions on the strength of a CFST column.
- Fig. 4(b)** indicates that L/D is negatively correlated with CFST strength, especially for long columns, which is also consistent with most references [51,71,126]. A stability factor (φ) in GB/T 51446 [24] and GB 50936 [25] is calculated through L/D so as to reflect the influence of slenderness on strength.
- The strength of a CFST column is more closely related to the individual sectional strengths of steel tube and core concrete components, rather than the material strengths of steel and concrete. Actually, in the database, for columns using high-strength materials, small-sized samples were usually designed due to the limitation of the testing facilities; whilst full-scale CFSTs generally adopted low- or mild-strength materials. Therefore, in order to comprehensively account for the sectional area (A_s , A_c) and the material strength (f_y , f_{cu}), secondary parameters, $f_y A_s$ and $f_{cu} A_c$, are adopted. It can be seen from **Fig. 4(b)** that both $f_y A_s$ and $f_{cu} A_c$ have a strong positive correlation with strength, with the r values over 0.86. These two secondary parameters are also adopted in most standards [20–25] to calculate the strength of CFST columns, as shown in **Table 5**.
- The correlations patterns between different parameters and the column strength are different for long and stub CFST columns. For example, secondary parameter $f_{cu} A_c$ has a correlation $r = 0.928$ with the strength of stub columns, much higher than that with the strength of long columns ($r = 0.864$). Similarly, $f_y A_s$ with $r = 0.898$ for stub columns is also higher than that with $r = 0.876$ for long

Table 4

Concrete information in literatures and the corresponding Pearson correlation coefficient (r).

	f'_c	f_{cu}	f_c
Type of concrete specimen	Cylinder	Cube	Prism
The number of measured strength in literatures	500	1110	159
Percentage to total measured strength	29.85%	66.27%	9.49%
r			
Global database	0.113	0.114	0.109
Stub-column database	0.028	0.03	0.025
Long-column database	0.27	0.271	0.27

Fig. 4. Pearson correlation coefficient (r) analysis of the basic/secondary parameters.

columns. This attributes to the fact that the failure mechanism of stub and long CFST columns exhibits significant difference, i.e., sectional strength failure for stub columns whilst overall buckling for long columns especially with large slenderness ratios [14,71, 126]. Additionally, long column is destroyed by the overall buckling, and the core concrete plays a major role in delaying the buckling of steel tube. Therefore, the material strength of concrete contributes less to the CFST strength, which becomes more obvious with the increase of slenderness ratio [14]. Correspondingly, $r = 0.876$ of f_yA_s for long column is higher than $r = 0.864$ of $f_{cu}A_c$, which once again shows that the steel tube of a long column is more crucial to the column strength due to its potential buckling.

- For the global, stub-column, and long-column databases, r between A_s and CFST strength is 0.928, 0.942, and 0.908, respectively, and these values are higher than the corresponding r of 0.891, 0.898, and 0.876 for f_yA_s . This phenomenon testifies that the contribution of steel tube to the strength of CFST columns acts not only through its sectional strength, but also through its confinement on the concrete core.

In summary, the parameters of long and stub CFST columns do not have the same correlation with strength, and secondary parameters have a greater correlation with strength than some basic parameters. For example, secondary parameters f_yA_s and $f_{cu}A_c$ have stronger positive correlation than corresponding basic parameters f_y and f_{cu} , while L/D also has generally higher correlation with strength than L for long columns. Combining the parameters used in existing standards and the results of correlation analysis, the influence of different parameters on the strength of CFST columns are comprehensively considered. Finally, five input parameters are rationally selected, namely D , t , L/D , f_yA_s and $f_{cu}A_c$, where, as introduced above, D and L are the sectional diameter and length of a CFST column; t , f_y , and A_s are the thickness, yield strength, and sectional area of steel tube, respectively; f_{cu} and A_c are the cube compressive strength and sectional area of concrete. Table 5 presents a comparison of the input parameters between the current ML methods and existing design standards. As can be seen in the table, the parameters selected in current study are highly consistent with those in these mainstream standards, demonstrating the reasonableness of the selected inputs.

4. Prediction performances of the established models

As reported in previous researches, most scholars used their database directly to train or test the ML models, without distinguishing the failure mechanisms between long and stub columns. It is expected that the laws between input parameters and strength would be to an extent related to the corresponding failure mechanisms. Therefore, it might not be effective to use one single ML model for the prediction of a wide range of CFST columns. In addition, the above correlation analysis proves that the influences of input parameters on long and stub columns are indeed different. Therefore, the established global database in this study is divided into stub-column and long-column databases, while the selected machine learning methods, namely BPNN, GA-BPNN, RBFNN, GPR and MLR, are attempted to predict the stub-column database, the long-column database, and the global database, respectively.

Table 5
Comparison of input parameters between the current methods and existing standards.

The current methods	International design standards					
	ACI 318 (2014) [20]	EC 4 (2004) [21]	AISC 360 (2016) [22]	AS/NZS 2327 (2017) [23]	GB/T 51446 (2021) [24]	GB 50936 (2014) [25]
D		✓	✓	✓		
t		✓	✓	✓		
L/D					✓	✓
f_yA_s	✓	✓	✓	✓	✓	✓
$f_{cu}A_c$	✓	✓	✓	✓	✓	✓

For each database, 90% of the collected test data is randomly selected for training, and the rest 10% is used for testing the capability of established model in predicting the axial strength of CFST columns. Detailed number of test samples in each database can be found in **Table 6**. As shown in **Fig. 3**, there are huge differences among the magnitudes and the ranges of variation of different parameters. Therefore, the parameters are all normalized between -1 and 1. All models are performed on Matlab R2020b [174]. For the current database containing 2,045 samples, the training and testing process for any of the above mentioned ML models are generally completed within 20 s, exhibiting excellent computational efficiency. When the process of model optimization is considered, the total computational cost is still much less than that of a detailed finite element method.

4.1. Evaluation index

In order to quantitatively compare the prediction performance of different models, six typical indexes for evaluating the model effectiveness are used.

1) Coefficient of determination (R^2),

$$R^2 = \frac{\left[\sum_{i=1}^n (\text{Exp}_i - \bar{\text{Exp}})(\text{Pre}_i - \bar{\text{Pre}}) \right]^2}{\left[\sum_{i=1}^n (\text{Exp}_i - \bar{\text{Exp}})^2 \right] \left[\sum_{i=1}^n (\text{Pre}_i - \bar{\text{Pre}})^2 \right]} \quad (4)$$

where Pre_i and Exp_i are the predicted strength and the experimental one, respectively; $\bar{\text{Exp}}$ is the average of the experimental strengths; and n is the total number of CFSTs in the specific set. R^2 is an index describing the correlation between the predicted strength and the experimental strength, which ranges from 0 to 1. The closer R^2 is to 1, the better the prediction performance.

2) Mean absolute error (MAE),

$$\text{MAE} = \frac{\sum_{i=1}^n |\text{Pre}_i - \text{Exp}_i|}{n} \quad (5)$$

MAE can avoid the problem that the over-estimating errors and the under-estimating ones cancel each other, so it can fairly reflect the actual prediction error.

3) Root mean square error (RMSE),

$$\text{RMSE} = \sqrt{\frac{\sum_{i=1}^n (\text{Pre}_i - \text{Exp}_i)^2}{n}} \quad (6)$$

RMSE is a frequently used index to compare the predicting errors between different models. Compared with MAE, the error is squared in RMSE so that a larger error is given a higher weight.

4) Mean absolute percentage error (MAPE),

$$\text{MAPE} = \frac{1}{n} \sum_{i=1}^n \frac{|\text{Pre}_i - \text{Exp}_i| \times 100\%}{\text{Exp}_i} \quad (7)$$

MAPE adopts the form of percentage which can averagely measure the prediction accuracy. A small set of values for MAE, RMSE and MAPE indicates a model with higher accuracy.

To facilitate comparison, two common statistical indexes, MEAN and COV, are also used to compare the error dispersion in different models.

5) Mean (MEAN),

$$\text{MEAN} = \frac{\sum_{i=1}^n (\text{Pre}_i / \text{Exp}_i)}{n} \quad (8)$$

6) Coefficient of variation (COV),

$$\text{COV} = \sqrt{\frac{\sum_{i=1}^n [(\text{Pre}_i / \text{Exp}_i) - \text{MEAN}]^2}{n}} \Bigg/ \text{MEAN} \quad (9)$$

Table 6

Number of test samples in the stub-column, long-column and global databases.

	Global database	Stub-column database (SCD)			Long-column database(LCD)		
		SCD	CS-1/RS-1	CS-2/RS-2	LCD	CS-1/RS-1	CS-2/RS-2
Training set	1841	1133	723	455	708	482	333
Testing set	204	126	80	50	78	53	37
Total	2045	1259	803	505	786	535	370

In this specific case, when MEAN is close to 1 while the COV value is small, the model is recognized as of high accuracy and low dispersion.

4.2. The adopted machine learning methods

4.2.1. BPNN and GA-BPNN

The back-propagation neural network (BPNN) was one of the widely used ML algorithms, which was initially devised by McCulloch and Pitts [175] and then developed by Rosenblatt [176]. A typical architecture of BPNN involves three portions: the input layer, the hidden layer, and the output layer. The main characteristics of BPNN are the following two phases: *i*) In the first phase, the inputs from the input layer are propagated forward through the network to generate outputs; *ii*) In the second phase, errors between actual value and generated outputs are propagated backward to modify weights and biases of the network. These two processes continue until the termination criterion is satisfied. A more detailed description of this algorithm can be found in Refs. [175,176]. The output from the j th neuron can be calculated as follows,

$$y_j = f(\text{net}_j) = f\left(\sum_{i=1}^n w_{ij}x_i + b_j\right) \quad (10)$$

where y_j is the output from the j th neuron; net_j is the summation generated at the j th neuron; w_{ij} is the weight from the i th neuron to j th neuron; x_i is the input from the i th neuron; b_j is the bias at the j th neuron; and f is the activation function including the log-sigmoid transfer function (Logsig), the tangent sigmoid transfer function (Tansig), and the linear transfer function (Purelin), etc.

Since the weights and biases are set to arbitrary values at first, BPNN could be trapped in local optimum and a global optimum may not be reached [177]. However, genetic algorithm (GA) has a strong global search ability based on Darwin's natural selection and evolution theory [178]. Combining GA with BPNN, GA is applied to optimize weights and biases of BPNN during training, so that the network achieves the goal of global optimization and efficiency. In order to highlight the effect of GA optimizing BPNN, the prediction performance between BPNN and GA-BPNN is compared in this study.

According to the characteristics of BPNN, 80% of the database is used for training, 10% for testing, and the remaining 10% for validating to monitor potential over-fitting. When BPNN begins to overfit the data, the error of validation data increases continuously. In this case, the training is stopped, and weights and biases return to the step where the over-fitting starts. It should be mentioned that the samples used for validating are counted in the training set when comparing the performance with other algorithms. One hidden layer is adopted and the topology of BPNN is set as 5-12-1 [174]. The activation function in the hidden layer and the output layer are taken as Tansig and Purelin, respectively. The training function is selected as Trainlm, which updates weights and biases as per Levenberg-Marquardt (L-M) algorithm. The BPNN process is terminated once the mean square error (MSE) is less than 0.0001 or the number of epochs reaches 2,000.

4.2.2. RBFNN

Although BPNN has been widely used in predicting the strength of structural members, it tends to show local optimization issue and relatively low training efficiency [178]. The radial basis function neural network (RBFNN) can overcome the above problems to some extent, and the network structure is simple so as to avoid lengthy computations. The typical architecture of RBFNN involves three portions: the input layer, the radial basis layer (RBL), and the linear layer (LL) [179,180]. The activation function in RBL is radial basis transfer function (Radbas), while Purelin is used in LL [174]. The outputs from RBL and LL are calculated as follows,

$$y_R = \text{radbas}(\text{dist}(w_R, x) \times b_R) \quad (11)$$

$$y_L = \text{purelin}(w_L y_R + b_L) \quad (12)$$

where y_R and y_L are outputs from RBL and LL, respectively; x is the input from the input layer; w_R and w_L are weights in RBL and LL, respectively; b_R and b_L are biases in RBL and LL.

There are two typical methods for establishing RBFNN [174]. One can establish a network with zero error on the training set, however, the drawback is that the number of neurons in RBL is the same as input vectors. Therefore, this method is not applicable when there are numerous input vectors. As for each iteration of the second method, only one input vector which can minimize the most network error is used as the neuron in RBL. If the error of the new network is less than the set error, the calculation is completed. Otherwise, the next neuron that minimizes the most network error is added. This process is repeated until the set error is met or the maximum number of neurons is reached. Therefore, the latter method is used in this paper, and spread is set to 0.45, 0.60, and 0.76 for stub-column, long-column, and global databases, respectively.

4.2.3. GPR

Gaussian process is a collection of random variables, any finite number of which have a joint Gaussian distribution [181]. It is completely specified by its mean function $m(x)$ and covariance function $k(x, x')$. The mean function and covariance function of a process $f(x)$ can be defined as,

$$m(x) = E[f(x)] \quad (13)$$

$$k(x, x') = E[(f(x) - m(x))(f(x') - m(x'))] \quad (14)$$

leaving the Gaussian process written as,

$$f(x) \sim GP(m(x), k(x, x')) \quad (15)$$

Gaussian process regression (GPR) is a specific method to apply Gaussian process theory on the field of regression analysis, where its complete description can be found in Ref. [181]. It is widely used to solve the high-dimensional, or non-linear problems. Compared with neural network, one advantage of GPR is that it can directly quantify the uncertainties of the prediction results.

4.2.4. MLR

For comparison purposes with the ML models, the multiple linear regression (MLR) method is utilized on the established database as well. The mathematical expression is assumed as follows,

$$N^{\text{MLR}} = a_1 D + a_2 t + a_3 L/D + a_4 f_y A_s + a_5 f_{cu} A_c + \epsilon \quad (16)$$

where a_i denotes a regression coefficient ($i = 1-5$) and ϵ represents an error term, both of which need to be determined by the regression.

4.3. Performance of the established models

Fig. 5 shows the distribution of errors obtained from BPNN and GA-BPNN models. For stub-column database, the accuracy of GA-BPNN is 42.89% for training set and 41.27% for testing set within an error range of 5%. These values are higher than those of 36.72% and 34.92% for BPNN. The accuracy of GA-BPNN for global database and long-column database are also better than BPNN, as shown in Fig. 5(a) and (c) respectively. The superior performance of GA-BPNN can be attributed to the optimal weights and biases with the aid of genetic algorithm. Therefore, it is feasible to utilize genetic algorithm to improve the performance of BPNN, and only GA-BPNN is used in the following analysis.

Fig. 6 demonstrates the prediction errors for GA-BPNN, RBFNN, GPR and MLR models, with the corresponding evaluation indexes summarized in Table 7. It can be observed in Fig. 6 that the highest accuracy of GPR for three databases is well recognized among three ML models, and more than 70% samples in the stub-column database are within 5% error range. The prediction accuracy between GA-BPNN and RBFNN exhibits little difference, and the dispersion of predictions is small with COV values less than 0.15. The performances of three ML models have a clear superiority in comparison with that of MLR, especially for long-column database as illustrated in Fig. 6 (c). In terms of testing set in long-column database, nearly 70% of predictions obtained from the three ML models have errors within 10%, whilst that for predictions by MLR is only 39.74%. As listed in Table 7, MLR can reasonably predict the strength of stub columns, with the R^2 for testing set of 0.988. However, for long columns, the value of R^2 for testing set drops to 0.912, with some predictions for columns with large slenderness ratios showing abnormal values. This again testifies that the hidden relationship between the strength of a long CFST column and its five input parameters is more complicated than that for a stub CFST column, clearly not as simple as a

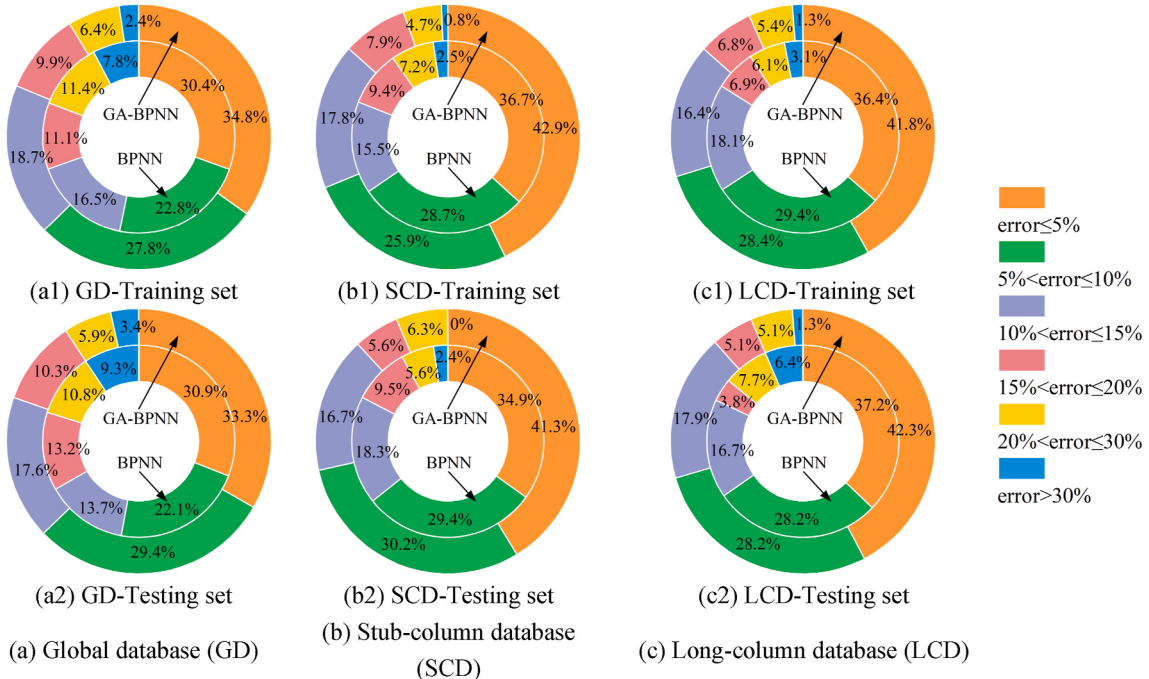


Fig. 5. Distribution of errors obtained from BPNN and GA-BPNN models.

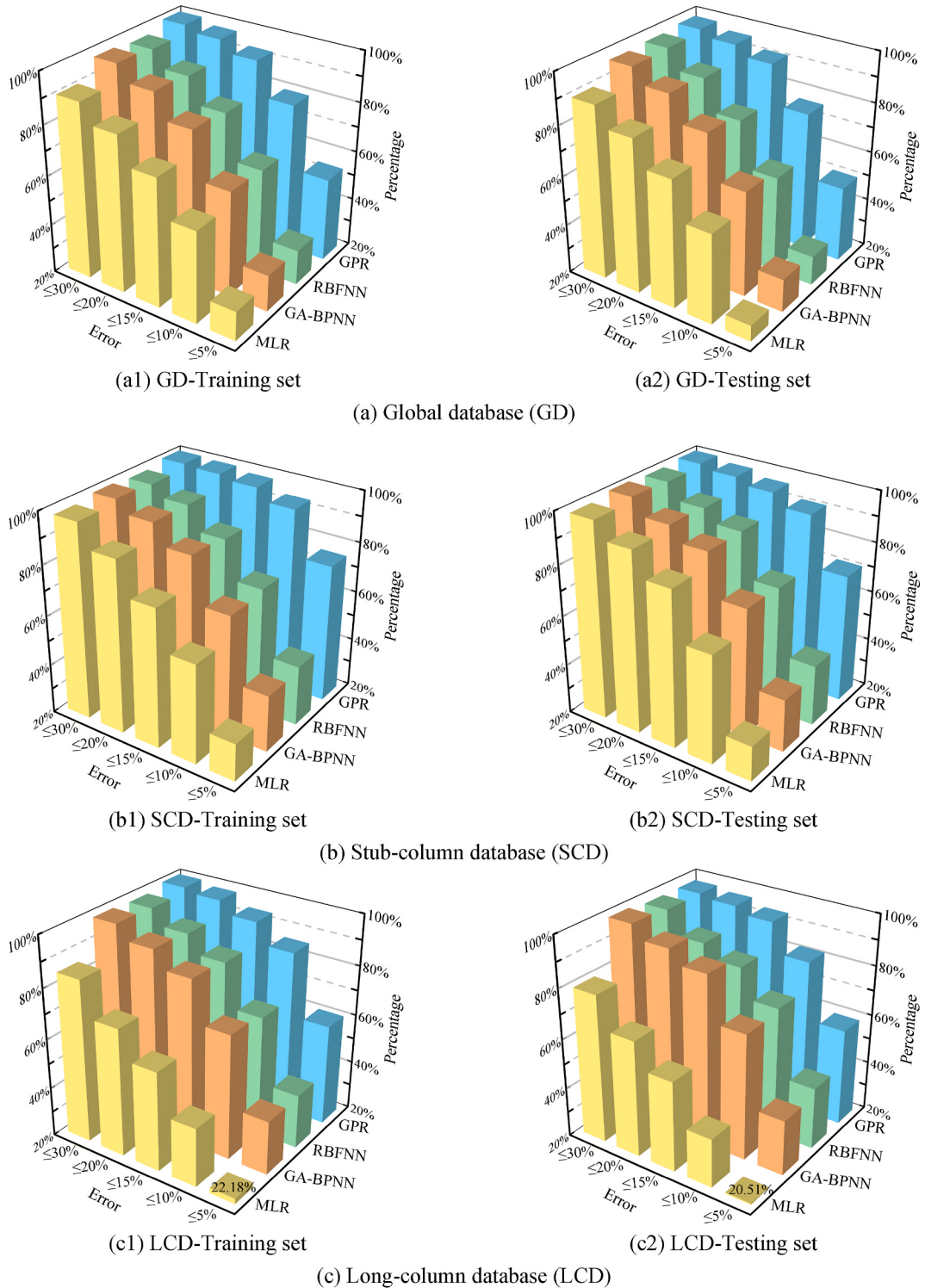


Fig. 6. Prediction errors for GA-BPNN, RBFNN, GPR and MLR models.

linear relationship. Fortunately, ML method is particularly suitable for exploring these complex nonlinear relationships, resulting in better predictions from the GA-BPNN, RBFNN and GPR models.

Compared with GA-BPNN and RBFNN, GPR not only has the highest prediction accuracy, but can also obtain the confidence intervals of the prediction results directly, as shown in Fig. 7. In this way, the uncertainty of prediction results can be quantified, which

Table 7
Evaluation results of the established four prediction models.

Model	Evaluation indexes	Global database		Stub-column database		Long-column database	
		Training set	Testing set	Training set	Testing set	Training set	Testing set
GA-BPNN	R^2	0.993	0.983	0.996	0.993	0.987	0.980
	MAE	175.941	178.392	175.336	166.665	95.232	90.857
	RMSE	294.256	306.856	261.656	239.841	152.022	171.873
	MAPE(%)	9.58%	9.98%	8.07%	7.62%	8.05%	7.89%
	MEAN	1.015	0.999	1.015	1.001	1.011	1.011
	COV	0.135	0.148	0.113	0.099	0.109	0.105
RBFNN	R^2	0.991	0.977	0.998	0.992	0.989	0.992
	MAE	190.509	200.290	152.563	165.269	92.127	74.812
	RMSE	339.407	346.641	212.797	261.192	141.990	106.410
	MAPE(%)	9.76%	10.34%	8.11%	7.58%	8.36%	8.35%
	MEAN	1.012	1.001	1.009	0.986	1.008	0.993
	COV	0.129	0.139	0.118	0.100	0.114	0.118
GPR	R^2	0.999	0.986	1.000	0.996	0.994	0.992
	MAE	88.062	136.546	62.868	103.108	61.426	62.217
	RMSE	133.693	270.308	92.497	186.409	105.637	105.705
	MAPE(%)	5.97%	6.99%	3.49%	4.38%	5.36%	6.05%
	MEAN	1.007	0.996	1.003	0.993	1.006	0.991
	COV	0.081	0.097	0.051	0.061	0.073	0.091
MLR	R2	0.972	0.954	0.976	0.988	0.938	0.912
	MAE	269.102	254.181	292.780	209.607	196.959	209.136
	RMSE	603.537	486.357	675.026	311.304	337.112	357.343
	MAPE(%)	15.47%	21.80%	9.95%	9.13%	19.51%	34.42%
	MEAN	0.955	0.880	0.991	0.978	0.949	0.786
	COV	0.365	0.676	0.132	0.117	0.410	1.079

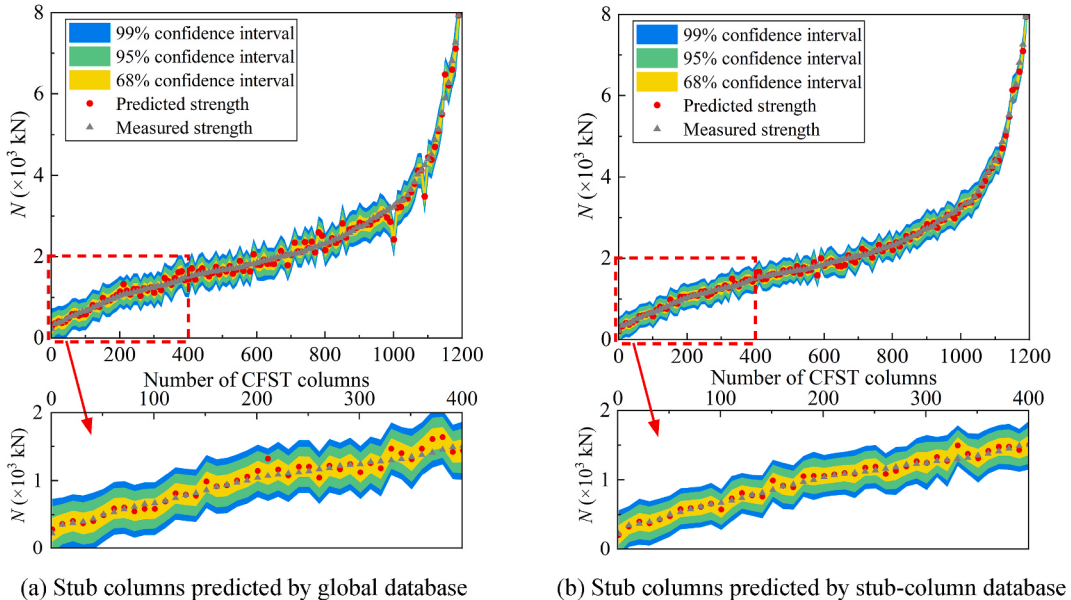


Fig. 7. Confidence intervals of GPR model.

stands more suitable to guide the practical design. In Fig. 7, the predicted strength of stub column is evenly distributed on both sides of the measured strength, which again testifies that GPR can accurately predict the strength of circular CFST columns.

4.4. Influence of database subdivision on the model performance

4.4.1. Database subdivision based on L/D

Previous studies have shown that long columns usually fail due to the loss of stability, whereas stub columns are mainly characterized by section failure [14,71,115]. Due to the huge difference between the failure mechanism of long and stub columns, the comparison of errors before and after database subdivision based on L/D is conducted, as presented in Fig. 8. It is apparent that for all three ML methods, the subdivision of long-column and stub-column databases helps achieve significantly improved accuracy compared to that using the global database, as can also be reflected from the evaluation indexes listed in Table 7. For example, as

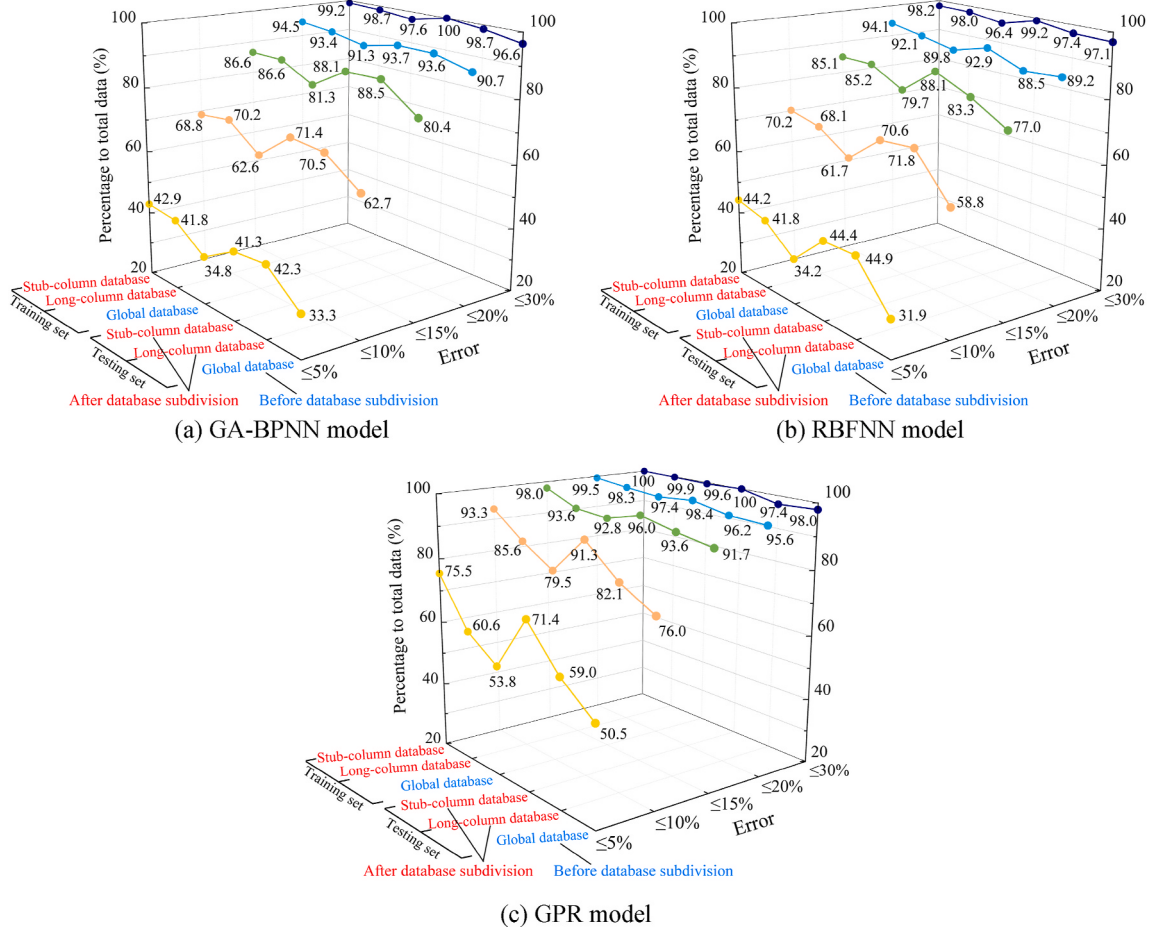


Fig. 8. Comparison of errors before and after database subdivision.

shown in Fig. 8, within the small error ranges (such as 5% and 10%), the proportion of samples in long-column or stub-column database is basically 6–21% larger than that in global database. Especially for GPR models, the proportion of training samples in the 5% error range increases from 53.83% for global database to 75.46% for stub-column database. Taking GA-BPNN as an example to predict the strength of long column, Fig. 9 shows the distribution of ratios between predicted strength to actual one under different ξ and L/D . Compared with ratios predicted by global database, more ratios predicted by long-column database are around 1, demonstrating that an improved performance of model is achieved through database subdivision based on L/D .

From a statistical point of view, Fig. 7(a) and (b) illustrates the confidence intervals of stub columns predicted by global and stub-column databases, respectively. It can be found from that the 68%, 95% and 99% confidence intervals predicted by global database are larger than the corresponding intervals obtained by stub-column database, indicating more effective predictions using the latter. This proves that the different failure mechanisms between long and stub CFST columns significantly affect the hidden relationship between the five inputs and the column strength. Therefore, it would be beneficial to subdivide a database according to failure mechanisms when adopting ML methods for structural predictions.

4.4.2. Further subdivision of database

In order to explore whether the accuracy of ML models can still be improved through further subdivision of the database, the database is further subdivided in this section other than the above attempt regarding L/D . Two kinds of subdivision methods are adopted: i) The database is subdivided according to certain conditions related to the structural mechanism of CFST columns, which is recorded as conditional subdivision (CS); ii) Samples are randomly selected from the database, which is recorded as random subdivision (RS). Both the long-column database and the stub-column database are subdivided twice by each method. CS-1 and CS-2 represent the first and second conditional subdivision, respectively. Similarly, RS-1 and RS-2 indicate the first and second random subdivision, respectively. Taking into account the randomness of random subdivision, RS-1 and RS-2 are performed five times respectively, and the average of five results is taken as the final accuracy. Detailed information of the subdivided database is shown in Table 6. After the second subdivision, the number of test samples in each database is larger than 350, indicating that the predicted results are still representative. It should be noted that the model is retrained after the database is subdivided.

For stub-column database, conditions of CS-1 are as follows: i) Given that the potential differences of testing rigs and loading/

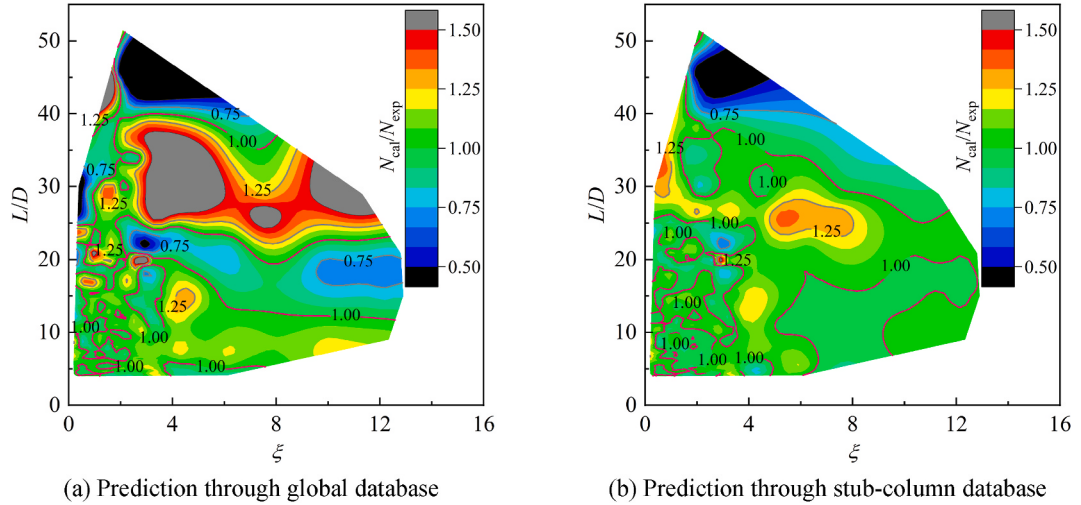


Fig. 9. Error distribution of long columns predicted by GA-BPNN models.

measuring methods in different eras may cause systematic errors in test data, only references published in the past 30 years (i.e. after 1990) are selected; ii) It is found from the above results that the strength prediction for CFSTs with non-practically small dimensions are unsatisfactory, which might due to the fact that when the cross-section of a CFST sample is too small, the compactness of concrete is

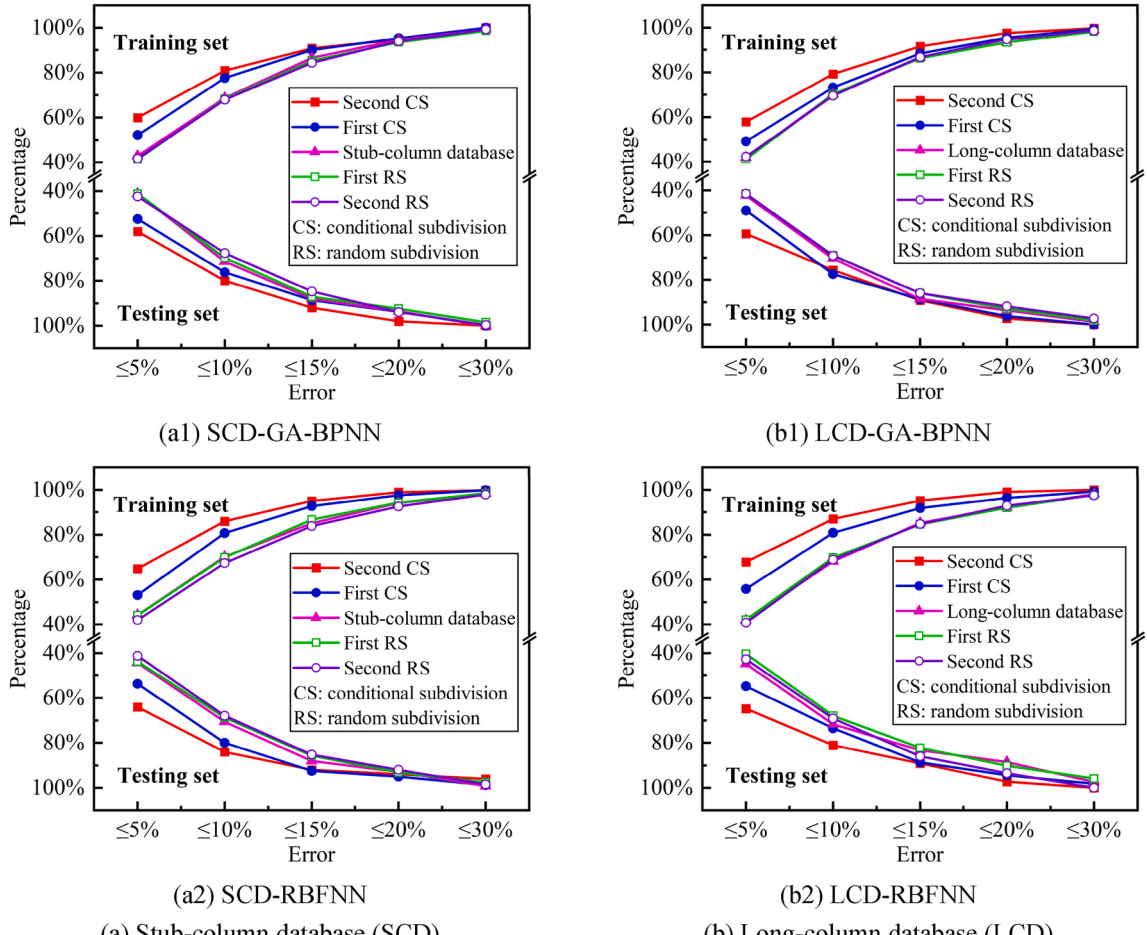


Fig. 10. Influence of database subdivision on the prediction accuracy.

an issue in manufacturing the test specimen. Therefore, CFST test samples with $D < 120$ mm or $f_{cu}A_c < 550$ kN are removed from the database. CS-2: On the basis of CS-1, the correlation between f_yA_s and N_{ue} is also found pronounced. As a further conditional subdivision, CFST test samples with $D < 130$ mm or $f_yA_s < 600$ kN are excluded from the database.

For long-column database, conditions of CS-1 are as follows: *i*) As shown in Fig. 9 (b), it is found from the above results that the prediction performances for CFSTs with non-practically large slenderness are unsatisfactory, which might due to the fact that the effects of potential initial imperfections during manufacturing become more sensitive for slender columns. Therefore, CFST test samples with $L/D \geq 25$ are removed from the database; *ii*) For the same reason stated above for stub-column database subdivisions, CFST test samples with $D < 90$ mm or $f_{cu}A_c < 300$ kN are removed from the database. CS-2: On the basis of CS-1, *i*) CFST test samples with $L/D \geq 15$ are excluded from the database; *ii*) CFST test samples with $f_yA_s < 300$ kN are removed from the database.

Taking GA-BPNN and RBFNN models as examples, Fig. 10 shows the influence of database subdivision methods on the prediction accuracy. As expected, the accuracy of both GA-BPNN and RBFNN models have been further improved after CS-1, especially in the ranges with smaller errors. For the large-error ranges, the models give a slight improvement compared with the ones before the conditional subdivision. More specifically, for the training set of stub-column database, when using GA-BPNN, the proportion of samples within 5% error range increased from 42.89% to 52.28%. For the testing set of long-column database, when using RBFNN, the proportion of samples within 5% error range increased from 44.87% to 54.72%. After CS-2, the accuracy has been further improved compared with that of CS-1. Taking the training set in stub-column database as an example, when using RBFNN, the percentage of CS-2 is 64.84% within the error range of 5%, whilst the corresponding percentage of CS-1 is 53.11%. With respect to each model and database after CS-2, the proportion of samples within 5% error range has increased from 41.27%-44.87% to 57.96%-67.87%, compared with the database before the conditional subdivision.

A comparison of accuracy between conditional and random subdivision is also plotted in Fig. 10. For the training set in stub-column database, when using GA-BPNN, the percentage of CS-1 is 52.28% within the error range of 5%, while corresponding percentages of five RS-1 attempts are 42.32%, 43.29%, 42.19%, 39.42%, and 40.11%, respectively. Different from conditional subdivision, the prediction accuracy of the models after random subdivision have not been significantly improved, sometimes even slightly lower than that of the model before subdivision. This shows that the model performance cannot be improved by randomly selecting the samples without mechanical consideration. When establishing the database, it is meaningful to clarify the difference in failure mechanisms and characteristics of the CFST test samples. In the above two subdivision methods, random subdivision has little or even adverse effect on the accuracy of ML model. If the database is divided according to certain conditions on the basis of mechanism analysis, a better accuracy can be achieved. Based on the above observation, it can be concluded that when applying ML methods in structural engineering sector, optimization of the models can be expected by rationally understanding the corresponding structural mechanisms.

5. Comparison between the established ML models and existing methods

Six commonly adopted design standards worldwide, namely ACI 318 [20], EC 4 [21], AISC 360 [22], AS/NZS 2327 [23], GB/T 51446 [24] and GB 50936 [25], are chosen to compare their prediction accuracy with the GA-BPNN, RBFNN and GPR models established in this paper. Two empirical formulas based on the ML methods developed by Tran et al. [173] and Zarringol et al. [11] are also adopted to compare the prediction performance.

5.1. Existing design standards

The database contains some CFST test samples of which the elastic modulus of steel (E_s) and concrete (E_c) are not reported in references, which need to be estimated using formulas in standards and references. According to AISC 360 [22] and Goode and Lam [45], 200 GPa is used for E_s when it is not given. Calculation formulas of E_c in different standards are not exactly the same, and the formula in EC 4 [21] is used in order to keep consistency. For comparative study, the limitations in the applicable ranges of each standard, as shown in Table 1, are ignored.

ACI 318 [20] considers the strength contribution of steel tube and concrete separately, therefore ignores the increase in the overall strength attributed from the material confinement. Unlike ACI 318 [20], EC 4 [21] considers the confinement effect besides the contribution of steel tube and concrete. In AISC 360 [22], CFST columns are categorized as compact, non-compact, and slenderness sections as per the section slenderness, and the strength of circular CFST sections is calculated in the above three cases. The applicable range of the recently updated AS/NZS 2327 [23] is relatively wider and its calculation principles for CFST columns are generally similar with those of EC 4 [21]. Based on the confinement theory, GB/T 51446 [24] adopts a confinement factor (ξ) to consider the composite action between steel tube and concrete. Moreover, a stability factor (ϕ) is employed to reflect the influence of slenderness on the axial strength of CFST columns. The design formulae derived through limit equilibrium method proposed in GB 50936 [25] have also been adopted in the calculation.

5.2. Empirical formulas in literatures

5.2.1. Tran's formula

Based on proposed artificial neural network, Tran et al. [173] established a simple empirical formula to calculate the axial compressive strength of circular CFST columns as follows,

$$N^{\text{Tran}} = (0.0462D^2 + 4.7889D + 88.876) C_L C_t C_{f_y} C_{f'_c} \quad (17)$$

where C_L , C_t , C_{f_y} , and $C_{f'_c}$ are the derived correction factors, with detailed reported in Ref. [173].

5.2.2. Zarringol's formula

Based on the activation functions used in BPNN model and weights and biases obtained from the trained BPNN model, Zarringol et al. [11] derived equations as follows,

$$N^{\text{Zarringol}} = \frac{65699}{1 + e^{Q_1}} - \frac{19828}{1 + e^{Q_2}} - \frac{26089}{1 + e^{Q_3}} - \frac{57486}{1 + e^{Q_4}} - \frac{67475}{1 + e^{Q_5}} + 92639 \quad (18)$$

where Q_1 - Q_5 are defined according to BPNN, the detailed formulas of which can be found in Ref. [11].

5.3. Comparison of the strength prediction models

The obtained predictions on the strength of circular CFST columns through the proposed ML models in this study are compared with those predicted by the above introduced design standards and empirical formulas, with the error distributions displayed in Figs. 11 and 12, respectively. Meanwhile, the comparisons between predicted and experimental strengths are illustrated in Fig. 13. Among the six standards considered, ACI 318 [20] is found the most conservative in predicting the strength of stub columns with a mean of 0.738, as shown in Fig. 13(a1). This is mainly due to the fact that it does not consider the increase in the overall strength attributed by the interaction between steel tube and concrete. At the meantime, its predictions on long columns are relatively discrete, with the highest standard deviation of 0.372. AISC 360 [22] gives conservative predictions for both long and stub columns with relatively smaller dispersion, which is consistent with the previous investigations [11,182]. It can be observed in Fig. 11 that the accuracy of GB/T 51446 [24] for long columns is well recognized, with the percentage of long-column database within an error range of 5% being 31.21% for the training set and 32.05% for the testing set. EC 4 [21] and AS/NZS 2327 [23] are also found effective for predicting the strength of stub columns. Taking the training set within an error range of 5% as an example, the percentages of stub-column database are 32.83% for EC 4 [21] and 33.36% for AS/NZS 2327 [23], respectively. In general, the accuracy of EC 4 [21], AS/NZS 2327 [23], GB/T 51446 [24] and GB 50936 [25] are comparable.

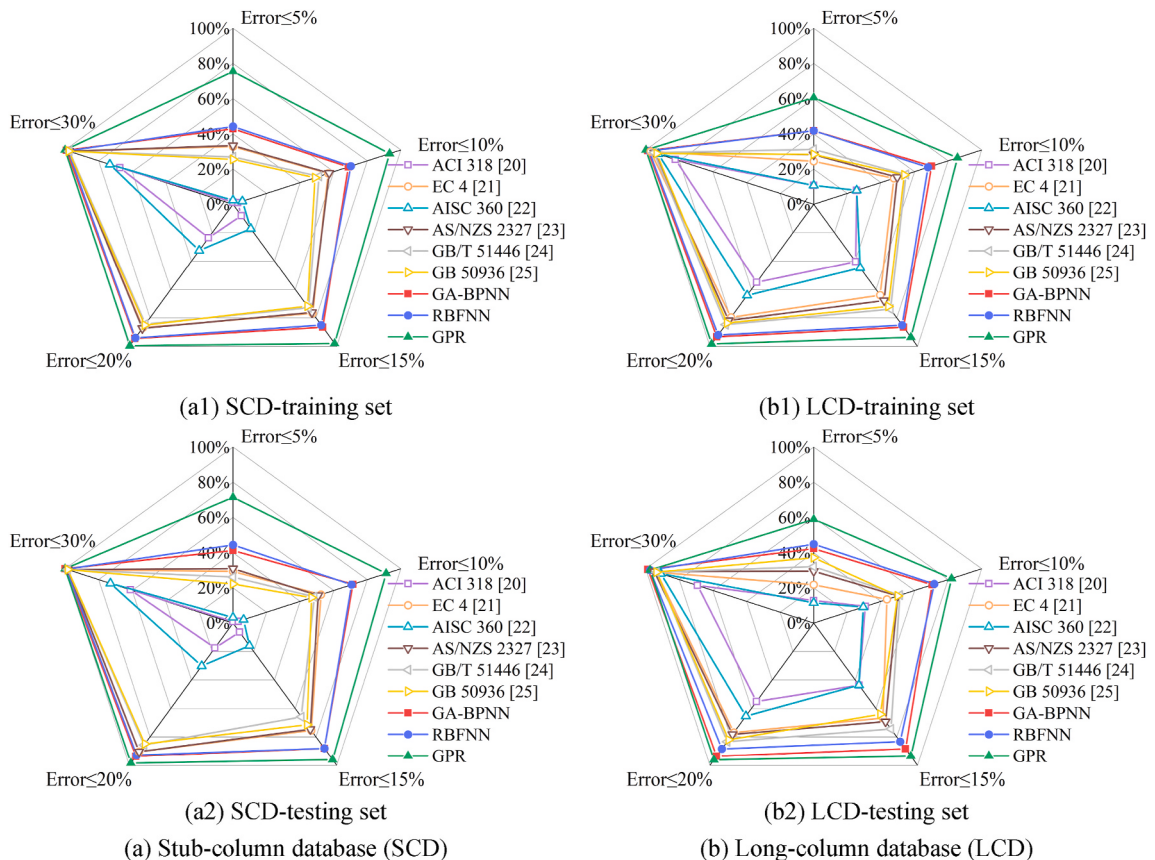


Fig. 11. Comparison between the proposed ML models and existing design standards.

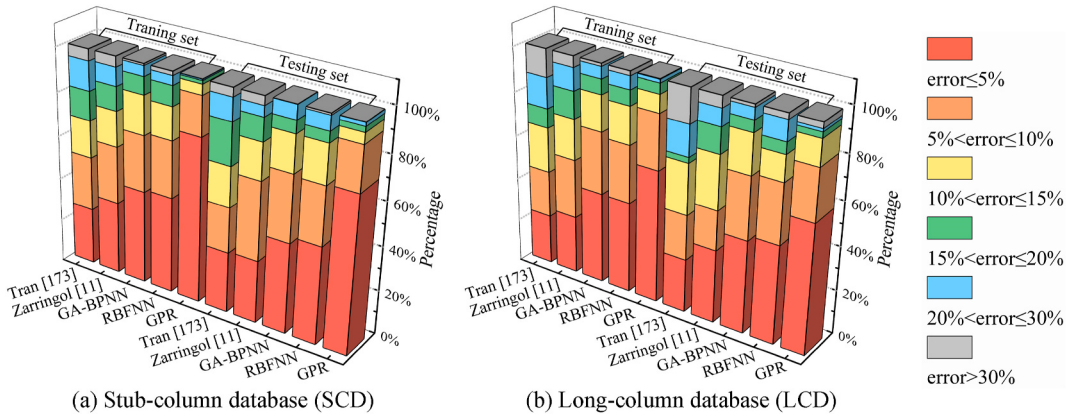


Fig. 12. Distribution of errors in the proposed ML models and empirical formulas.

As can be seen from Figs. 11 and 13, the accuracy of the GA-BPNN, RBFNN and GPR models proposed in this paper are obviously superior than those of the six design standards, especially for the proportion of the predictions within a small error range. For instance, 70.20%, 68.08% and 85.59% of long-column database of training set obtained from GA-BPNN, RBFNN and GPR models show error within 10%, much higher than the 25.56%, 47.74%, 25.56%, 49.72%, 54.95% and 53.95% proportions calculated by ACI 360 [20], EC 4 [21], AISC 360 [22], AS/NZS 2327 [23], GB/T 51446 [24] and GB 50936 [25], respectively. For both the stub-column and the long-column databases, the standard deviations of three ML models are no more than 0.118, exhibiting low dispersions. The superiority of the established ML methods in predicting the axial compression strength of circular CFST columns can be well recognized.

In terms of the comparison between the current models and those proposed by Tran et al. [173] and Zarringol et al. [11], as shown in Fig. 12, the accuracy of ML models in this study are the highest. The reason to this can be attributed to two main facts, firstly, the current database is the largest within the three studies, containing 2,045 CFST test samples; secondly, optimization through database subdivision is adopted according to failure mechanisms of CFST columns. From the perspective of dispersion, the GA-BPNN, RBFNN and GPR models proposed in this paper are significantly smaller than two previous empirical formulas as well, as shown in Fig. 13.

6. Conclusion

Based upon a collected database composed of 2,045 circular CFST columns under axial compression, mainstream machine learning methods BPNN, GA-BPNN, RBFNN, GPR as well as MLR models have been established for predicting the strength of CFST columns. The prediction effectiveness of the established models are compared with existing design standards and previous empirical formulas. The following conclusions can be drawn.

- (1) The proposed GA-BPNN and RBFNN models, especially GPR models, can accurately and reliably predict the strengths of circular CFST columns. Compared with existing standards and empirical formulas, the three ML models proposed in this study have shown better performance and wider applicable range.
- (2) The main parameters of long and stub CFST columns are found to have different correlation patterns with the column strength. It indicates that correlation analysis and mechanism analysis are necessary to help identify input factors when adopting machine learning methods for structural design.
- (3) Compared with BPNN, using genetic algorithm to optimize weights and biases of BPNN can improve the prediction performance. MLR has higher accuracy for stub-column database than long-column database, which indicates that the failure mechanism of long column is more complicated and shows more nonlinear patterns.
- (4) The accuracy of the established GA-BPNN, RBFNN and GPR models on long-column or stub-column databases are all better than those of global database, indicating that it is effective to divide CFST columns according to the failure mechanism. The prediction accuracies are further improved when the database continues to be subdivided in accordance with certain conditions regarding mechanism analysis, whilst random subdivision of the database has little or even adverse effect on the model accuracy.

CRediT author statement

Chao Hou: Conceptualization, Methodology, Supervision, Investigation, Writing - Review & Editing. **Xiaoguang Zhou:** Methodology, Investigation, Data Curation, Writing - Original draft.

Declaration of competing interest

The authors declare that they have no known competing financial interests or personal relationships that could have appeared to influence the work reported in this paper.

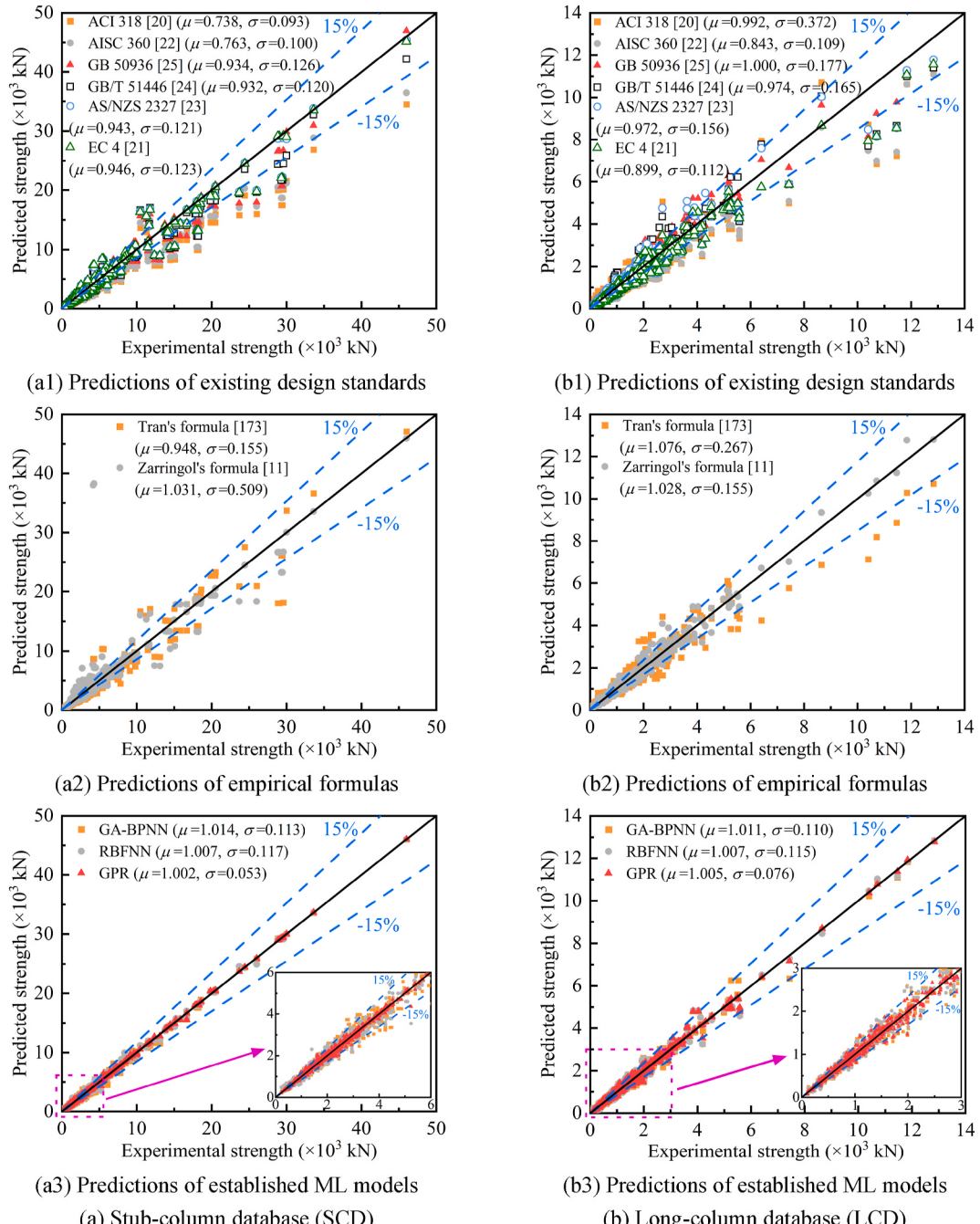


Fig. 13. Comparison between the predicted and experimental strengths
Notes: μ represents the mean; σ represents the standard deviation.

Acknowledgements

The research reported in this paper is supported by the Shenzhen Science and Technology Innovation Commission (No. 20200925154412003) and Southern Marine Science and Engineering Guangdong Laboratory (Guangzhou) (No. K19313901). The financial support is highly appreciated. The authors also greatly appreciate the open database provided by Professor C. Douglas Goode and Professor Dennis Lam in Reference [45].

References

- [1] T. Jo, Machine Learning Foundations: Supervised, Unsupervised, and Advanced Learning, Springer, 2021.
- [2] A. Behnood, V. Behnood, M.M. Gharehveran, et al., Prediction of the compressive strength of normal and high-performance concretes using MSP model tree algorithm, *Construct. Build. Mater.* 142 (2017) 199–207.
- [3] Z.H. Duan, S.C. Kou, C.S. Poon, Prediction of compressive strength of recycled aggregate concrete using artificial neural networks, *Construct. Build. Mater.* 40 (2013) 1200–1206.
- [4] H. Nguyen, T. Vu, T.P. Vo, et al., Efficient machine learning models for prediction of concrete strengths, *Construct. Build. Mater.* 266 (2021) 120950.
- [5] E.M. Golafshani, A. Behnood, Application of soft computing methods for predicting the elastic modulus of recycled aggregate concrete, *J. Clean. Prod.* 176 (2018) 1163–1176.
- [6] N. Ceryan, E.C. Ozkat, N.K. Can, et al., Machine learning models to estimate the elastic modulus of weathered magmatic rocks, *Environ. Earth Sci.* 80 (2021) 448.
- [7] S. Mangalathu, H. Jang, S.H. Hwang, et al., Data-driven machine-learning-based seismic failure mode identification of reinforced concrete shear walls, *Eng. Struct.* 208 (2020) 110331.
- [8] S. Mangalathu, J.S. Jeon, Machine learning-based failure mode recognition of circular reinforced concrete bridge columns: comparative study, *J. Struct. Eng.* 145 (10) (2019), 04019104.
- [9] O.B. Olalusi, P.O. Awoyera, Shear capacity prediction of slender reinforced concrete structures with steel fibers using machine learning, *Eng. Struct.* 227 (2021) 111470.
- [10] V.L. Tran, D.K. Thai, S.E. Kim, Application of ANN in predicting ACC of SCFST column, *Compos. Struct.* 228 (2019) 111332.
- [11] M. Zarringol, H.T. Thai, S. Thai, et al., Application of ANN to the design of CFST columns, *Structures* 28 (2020) 2203–2220.
- [12] Q.V. Vu, V.H. Truong, H.T. Thai, Machine learning-based prediction of CFST columns using gradient tree boosting algorithm, *Compos. Struct.* 259 (2021) 113505.
- [13] Z.U.R. Tahir, P. Mandal, Artificial neural network prediction of buckling load of thin cylindrical shells under axial compression, *Eng. Struct.* 152 (2017) 843–855.
- [14] L.H. Han, Concrete Filled Steel Tubular Structures-Theory and Practice, third ed., Science Press, Beijing, China, 2016 (in Chinese).
- [15] S.P. Schneider, Axially loaded concrete-filled steel tubes, *J. Struct. Eng.* 124 (10) (1998) 1125–1138.
- [16] Z.P. Chen, J.J. Xu, Y.L. Chen, et al., Recycling and reuse of construction and demolition waste in concrete-filled steel tubes: a review, *Construct. Build. Mater.* 126 (2016) 641–660.
- [17] S.D. Nardin, A.L.H.C.E. Debs, Axial load behaviour of concrete-filled steel tubular columns, *Structures and Buildings* 159 (SB1) (2007) 13855.
- [18] L.H. Han, W. Li, R. Bjørhovde, Developments and advanced applications of concrete-filled steel tubular (CFST) structures: Members, *J. Constr. Steel Res.* 100 (2014) 211–228.
- [19] J.G. Wei, X. Luo, Z.C. Lai, et al., Experimental behavior and design of high-strength circular concrete-filled steel tube short columns, *J. Struct. Eng.* 146 (1) (2020), 04019184.
- [20] ACI 318, Building Code Requirements for Structural Concrete (ACI 318-14) and Commentary (ACI 318R-14), American Concrete Institute, Detroit, USA, 2014.
- [21] Eurocode 4, Design of Composite Steel and Concrete Structures-Part 1.1: General Rules and Rules for Buildings (EC 4-2004), European Committee for Standardization, British Standards Institution, London, UK, 2004.
- [22] AISC 360, Specification for Structural Steel Buildings (AISC 360-16), American Institute of Steel Construction, Chicago, USA, 2016.
- [23] AS/NZS 2327, Composite Structures-Composite Steel-Concrete Construction in Buildings (AS/NZS 2327-2017), Standards Australia/New Zealand Committee, 2017. Sydney/Wellington, Australia/New Zealand.
- [24] GB/T 51446, Technical Standard for Concrete-Filled Steel Tubular Hybrid Structures (GB/T 51446-2021), Ministry of Housing and Urban-Rural Development of the People's Republic of China, Beijing, China, 2021.
- [25] GB 50936, Technical Code for Concrete Filled Steel Tubular Structures (GB 50936-2014), Ministry of Housing and Urban-Rural Development of the People's Republic of China, Beijing, China, 2014.
- [26] L.H. Han, Tests on concrete filled steel tubular columns with high slenderness ratio, *Adv. Struct. Eng.* 3 (4) (2000) 337–344.
- [27] M.X. Xiong, D.X. Xiong, J.Y.R. Liew, Axial performance of short concrete filled steel tubes with high- and ultra-high- strength materials, *Eng. Struct.* 136 (2017) 494–510.
- [28] Q.X. Ren, L.H. Han, D. Lam, et al., Experiments on special-shaped CFST stub columns under axial compression, *J. Constr. Steel Res.* 98 (2014) 123–133.
- [29] Y.E. Hao, Z.D. Zhai, Evaluation of axial bearing capacity of filling steel tube concrete columns with rectangular section, *J. Chang'an Univ. (Nat. Sci. Ed.)* 21 (3) (2004) 24–28 (in Chinese).
- [30] H.G. Gao, H.J. Wang, X.Q. Li, Investigation on bearing capacity of square CFT columns under axial load based on neural network, *Journal of Shenyang University of technology* 27 (6) (2005) 678–681 (in Chinese).
- [31] M.C. Zhu, Q.X. Wang, X.F. Feng, Prediction of axial capacity of concrete-filled square steel tubes using neural networks, *J. Southwest Jiatot. Univ.* 13 (2) (2005) 151–155.
- [32] H.J. Wang, H.B. Zhu, H. Wei, Bearing capacity of concrete filled square steel tubular columns based on neural network, *Adv. Mater. Res.* 502 (2012) 193–197.
- [33] H.G. Gao, Calculation of load-carrying capacity of square concrete filled tube columns based on neural network, *Appl. Mech. Mater.* 71–78 (2011) 847–850.
- [34] A. Kheyroddin, H. Naderpour, M. Ahmadi, Performance of Circular Concrete Filled Steel Tube Members Subjected to Axial Load, 4th International Conference on Concrete and Development, Tehran, Iran, 2013.
- [35] V.L. Tran, D.K. Thai, D.D. Nguyen, Practical artificial neural network tool for predicting the axial compression capacity of circular concrete-filled steel tube columns with ultra-high-strength concrete, *Thin-Walled Struct.* 151 (2020) 106720.
- [36] A.I. Nour, E.M. Güneyisi, Prediction model on the compressive strength of recycled aggregate concrete filled steel tube columns, *Composites Part B* 173 (2019) 106938.
- [37] J.J. Xu, Y.M. Wang, R. Ren, et al., Performance evaluation of recycled aggregate concrete-filled steel tubes under different loading conditions: database analysis and modelling, *J. Build. Eng.* 30 (2020) 101308.
- [38] M. Ahmadi, H. Naderpour, A. Kheyroddin, Utilization of artificial neural networks to prediction of the capacity of CCFT short columns subject to short term axial load, *Archives of Civil and Mechanical Engineering* 14 (2014) 510–517.
- [39] E.M. Güneyisi, A. Gültekin, K. Mermerdaş, Ultimate capacity prediction of axially loaded CFST short columns, *International Journal of Steel Structures* 16 (1) (2016) 99–114.
- [40] M.Z. Naser, S. Thai, H.T. Thai, Evaluating structural response of concrete-filled steel tubular columns through machine learning, *J. Build. Eng.* 34 (2021) 101888.
- [41] H.Q. Nguyen, H.B. Ly, V.Q. Tran, et al., Optimization of artificial intelligence system by evolutionary algorithm for prediction of axial capacity of rectangular concrete filled steel tubes under compression, *Materials* 13 (2020) 1205.
- [42] Y.S. Du, Z.H. Chen, C.Q. Zhang, et al., Research on axial bearing capacity of rectangular concrete-filled steel tubular columns based on artificial neural networks, *Front. Comput. Sci.* 11 (2016) 863–873.
- [43] Q.Y. Zhang, Z.H. Chen, X.D. Wang, Calculation method of high strength concrete-filled rectangular steel tubular columns based on artificial neural networks, *Journal of Shijiazhuang Tiedao University (Natural Science Edition)* 31 (1) (2018) 11–15 (in Chinese).
- [44] GB 50010, Code for Design of Concrete Structures (GB 50010-2010), Ministry of Housing and Urban-Rural Development of the People's Republic of China, Beijing, China, 2010 (in Chinese).
- [45] C.D. Goode, D. Lam, Concrete-filled Steel Tube Columns-Tests Compared with Eurocode 4, Composite Construction VI, Colorado, USA, 2008.

- [46] GB/T 50081, Standard for Test Methods of Concrete Physical and Mechanical Properties (GB/T 50081-2019), Ministry of Housing and Urban-Rural Development of the People's Republic of China, Beijing, China, 2019 (in Chinese).
- [47] K. Sakino, H. Nakahara, S. Morino, et al., Behavior of centrally loaded concrete-filled steel-tube short columns, *J. Struct. Eng.* 130 (2) (2004) 180–188.
- [48] C.S. Huang, Y.K. Yeh, G.Y. Liu, et al., Axial load behavior of stiffened concrete-filled steel columns, *J. Struct. Eng.* 128 (9) (2002) 1222–1230.
- [49] B. Li, R.X. Hao, The analysis of concrete filled steel tube column carrying capacity, *Journal of Baotou University of Iron and Steel Technology* 24 (1) (2005) 5–8 (in Chinese).
- [50] L.H. Han, Theoretical analysis and experimental researches for the behaviors of high strength concrete filled steel tubes subjected to axial compression, *Ind. Constr.* 27 (11) (1997) 39–44+13.
- [51] J. Zeghiche, K. Chaoui, An experimental behaviour of concrete-filled steel tubular columns, *J. Constr. Steel Res.* 61 (2005) 53–66.
- [52] M.D. O'Shea, R.Q. Bridge, Design of circular thin-walled concrete filled steel tubes, *J. Struct. Eng.* 126 (11) (2000) 1295–1303.
- [53] B. Li, Y. Wen, Experimental study on bearing capacity of long concrete filled steel tubular columns with axial compression, *Earthq. Eng. Eng. Vib.* 23 (5) (2003) 130–133.
- [54] L.H. Han, S.F. Jiang, Y.Q. Cao, et al., Experimental studies on the behavior and strength of very slender concrete filled steel tubular columns, *Steel Construction* 14 (44) (1999) 21–25.
- [55] B. Kato, Column curves of steel-concrete composite members, *J. Constr. Steel Res.* 39 (2) (1996) 121–135.
- [56] S. Ghannam, Y.A. Jawad, Y. Hunait, Failure of lightweight aggregate concrete-filled steel tubular columns, *Steel Compos. Struct.* 4 (1) (2004) 1–8.
- [57] L.H. Han, G.H. Yao, Z.B. Chen, et al., Experimental behaviours of steel tube confined concrete (STCC) columns, *Steel Compos. Struct.* 5 (6) (2005) 459–484.
- [58] H.G.L. Prion, J. Boehme, Beam-column behaviour of steel tubes filled with high strength concrete, *Can. J. Civ. Eng.* 21 (1994) 207–218.
- [59] K.F. Tan, X.C. Pu, Study on behavior and load bearing capacities of slender steel tubular columns and eccentrically loaded steel tubular columns filled with extra-high strength concrete, *J. Build. Struct.* 21 (2) (2000) 12–19.
- [60] M.N. Baig, J.S. Fan, J.G. Nie, Strength of concrete filled steel tubular columns, *Tsinghua Sci. Technol.* 11 (6) (2006) 657–666.
- [61] L.H. Han, G.H. Yao, X.L. Zhao, Tests and calculations for hollow structural steel (HSS) stub columns filled with self-consolidating concrete (SCC), *J. Constr. Steel Res.* 61 (2005) 1241–1269.
- [62] M. Johansson, The efficiency of passive confinement in CFT columns, *Steel Compos. Struct.* 2 (5) (2002) 379–396.
- [63] V.W.Y. Tam, J.Z. Xiao, S. Liu, et al., Behaviors of recycled aggregate concrete-filled steel tubular columns under eccentric loadings, *Front. Struct. Civ. Eng.* 13 (3) (2019) 628–639.
- [64] Y.Y. Wang, S.M. Zhang, Individual behavior of steel tube and concrete in CFST stub columns subjected to axial compression, *J. Harbin Inst. Technol.* 35 (S) (2003) 31–34 (in Chinese).
- [65] S.M. Zhang, J.P. Liu, L. Ma, et al., Axial compression test and analysis of circular tube confined HSC stub columns, *China Civ. Eng. J.* 40 (3) (2007) 24–31+68.
- [66] S.K. Alrebeh, T. Ekmekyapar, Structural behavior of concrete-filled steel tube short columns stiffened by external and internal continuous spirals, *Structures* 22 (2019) 98–108.
- [67] M.X. Xiong, D.X. Xiong, J.Y.R. Liew, Behaviour of steel tubular members infilled with ultra high strength concrete, *J. Constr. Steel Res.* 138 (2017) 168–183.
- [68] Q.X. Ren, K. Zhou, C. Hou, et al., Dune sand concrete-filled steel tubular (CFST) stub columns under axial compression: Experiments, *Thin-Walled Struct.* 124 (2018) 291–302.
- [69] G.C. Chen, Z.S. Xu, Z.S. Yang, et al., Experimental study on behavior of short steel tubular columns filled with ultra-high strength concrete mixed with stone-chip subjected to axial load, *J. Build. Struct.* 32 (3) (2011) 82–89.
- [70] L.M. Ma, S.W. Li, L. Zhu, et al., Experimental study on axial compression behavior of concrete filled high strength circular steel tubular short columns, *Ind. Constr.* 16 (7) (2016) 16–21.
- [71] T. Ekmekyapar, B.J.M. Al-Eliwi, Experimental behaviour of circular concrete filled steel tube columns and design specifications, *Thin-Walled Struct.* 105 (2016) 220–230.
- [72] A.T. Beck, W.L.A.D. Oliveira, S.D. Nardim, et al., Reliability-based evaluation of design code provisions for circular concrete-filled steel columns, *Eng. Struct.* 31 (2009) 2299–2308.
- [73] J.Y.R. Liew, D.X. Xiong, Effect of preload on the axial capacity of concrete-filled composite columns, *J. Constr. Steel Res.* 65 (2009) 709–722.
- [74] Z.W. Yu, F.X. Ding, C.S. Cai, Experimental behavior of circular concrete-filled steel tube stub columns, *J. Constr. Steel Res.* 63 (2007) 165–174.
- [75] K.F. Tan, L.B. Liu, Mechanical properties of high strength concrete filled steel tubular columns, *Adv. Mater. Res.* 472–475 (2012) 1119–1125.
- [76] X.J. Zhou, T.M. Mou, H.Y. Tang, et al., Experimental study on ultrahigh strength concrete filled steel tube short columns under axial load, *Adv. Mater. Sci. Eng.* 2017 (2017) 8410895.
- [77] Y.Y. Wang, P. Chen, C.Y. Liu, et al., Size effect of circular concrete-filled steel tubular short columns subjected to axial compression, *Thin-Walled Struct.* 120 (2017) 397–407.
- [78] W.J. Wang, H. Ma, Z.B. Li, et al., Size effect in circular concrete-filled steel tubes with different diameter-to-thickness ratios under axial compression, *Eng. Struct.* 151 (2017) 554–567.
- [79] X.J. Ke, Z.P. Chen, W.D. Ying, et al., Experimental study on the axial compression performance of high-strength concrete filled steel tube columns, *Building Structure* 44 (16) (2014) 46–49+76.
- [80] P. Chen, Y.Y. Wang, C.Y. Liu, et al., Experimental study on size effect of circular concrete-filled steel tubular columns subjected to axial compression, *J. Build. Struct.* 38 (S1) (2017) 249–257.
- [81] F. Abed, M. Alhamaydeh, S. Abdalla, Experimental and numerical investigations of the compressive behavior of concrete filled steel tubes (CFSTs), *J. Constr. Steel Res.* 80 (2013) 429–439.
- [82] T. Yamamoto, J. Kawaguchi, S. Morino, Experimental study of the size effect on the behaviour of concrete filled circular steel tube columns under axial compression, *Journal of Structural and Construction Engineering* 561 (2002) 237–244 (in Japanese).
- [83] Z.W. Yu, F.X. Ding, S. Lin, Researches on behavior of high-performance concrete filled tubular steel short columns, *J. Build. Struct.* 23 (2) (2002) 41–47.
- [84] N.J. Gardner, E.R. Jacobson, Structural behavior of concrete filled steel tubes, *J. Am. Concr. Inst.* 64 (7) (1967) 404–413.
- [85] F. He, X.H. Zhou, C.H. Tang, Experimental research on the bearing behavior of high-strength-concrete-filled steel tube under axial compression, *Eng. Mech.* 17 (4) (2000) 61–66.
- [86] M. Abramski, Load-carrying capacity of axially loaded concrete-filled steel tubular columns made of thin tubes, *Archives of Civil and Mechanical Engineering* 18 (3) (2018) 902–913.
- [87] S.M. Zhou, Q. Sun, X.H. Wu, Impact of D/t ratio on circular concrete-filled high-strength steel tubular stub columns under axial compression, *Thin-Walled Struct.* 132 (2018) 461–474.
- [88] B. Kato, Compressive strength and deformation capacity of concrete-filled tubular stub columns, *Journal of Structural and Construction Engineering* 468 (1995) 183–191 (in Japanese).
- [89] J.Q. Xue, B. Briseghella, B.C. Chen, Effects of debonding on circular CFST stub columns, *J. Constr. Steel Res.* 69 (2012) 64–76.
- [90] M.H. Lai, J.C.M. Ho, A theoretical axial stress-strain model for circular concrete-filled-steel-tube columns, *Eng. Struct.* 125 (2016) 124–143.
- [91] M. Saisho, T. Abe, K. Nakaya, Ultimate bending strength of high-strength concrete filled steel tube column, *Journal of Structural and Construction Engineering* 523 (1999) 133–140 (in Japanese).
- [92] W. Gu, C.W. Guan, Y.H. Zhao, et al., Experimental study on concentrically-compressed circular concrete filled CFRP-steel composite tubular short columns, *Journal of Shenyang Architecture and Civil Engineering University* 20 (2) (2004) 118–120 (in Chinese).
- [93] Y.M. Hu, T. Yu, J.G. Teng, FRP-confined circular concrete-filled thin steel tubes under axial compression, *J. Compos. Construct.* 15 (5) (2011) 850–860.
- [94] F.Y. Liao, L.H. Han, S.H. He, Behavior of CFST short column and beam with initial concrete imperfection: Experiments, *J. Constr. Steel Res.* 67 (2011) 1922–1935.

- [95] Y.J. Li, L.H. Han, W. Xu, et al., Circular concrete-encased concrete-filled steel tube (CFST) stub columns subjected to axial compression, *Mag. Concr. Res.* 68 (19) (2016) 995–1010.
- [96] H. Huang, X.Y. Guo, M.C. Chen, et al., Comparative experimental research on concrete-filled steel tubular columns subjected to axial compression, *J. Guangxi Univ. (Nat. Sci. Ed.)* 40 (4) (2015) 806–814 (in Chinese).
- [97] J.H. Zhao, Q. Gu, S.F. Ma, The study of the axial compressive strength of concrete filled steel tube (CFST) based on the twin shear unified strength theory, *Eng. Mech.* 19 (2) (2002) 32–35.
- [98] Y. Li, M.S. Zhan, J.G. Xiong, Experimental research on properties of concrete filled thin walled steel tube column under axial compression, *J. Nanchang Univ. (Eng. Technol.)* 31 (1) (2009) 99–102 (in Chinese).
- [99] B.Z. Cao, Y.C. Zhang, Q.P. Wang, et al., Mechanical behavior of circular concrete filled thin-walled steel tube stub columns, *J. Harbin Inst. Technol.* 37 (S) (2005) 141–144 (in Chinese).
- [100] P.H. Ning, X.P. Li, M. Xiao, Experimental study on bearing capacity of concrete-filled steel tubular members under axial compression, *Highways* (9) (2004) 53–56.
- [101] Q.Y. Cui, Y. Zhang, Researches on the mechanics behavior of concrete filled steel tubular columns, *Building Science research of Sichuan* 29 (1) (2003) 19–21 (in Chinese).
- [102] Z. Wang, Experimental Research on Mechanical Property of Circular Concrete-Filled Thin-Walled Steel Tubular Column under Axial Load, Harbin Institute of Technology, Harbin, 2016 (in Chinese).
- [103] Y. Li, X.L. Tang, Experiment of axial bearing capacity steel tubular of self-compacting concrete-filled columns, *Journal of Architecture and Civil Engineering* 25 (3) (2008) 26–31.
- [104] F.J. Zhang, J.W. Xia, H.F. Chang, et al., Ultimate strength analysis to thin-walled circular concrete-filled steel tube column under axial compression, *Concrete* (7) (2015) 18–21.
- [105] L.S. Wang, J.R. Qian, Experimental study on axial compression bearing capacity of high strength concrete-filled steel tubular columns, *Building Structures* 33 (7) (2003) 46–49.
- [106] Y. Che, Q.L. Wang, Y.B. Shao, Compressive performances of the concrete filled circular CFRP-steel tube (C-CFRP-CFST), *Advanced Steel Construction* 8 (4) (2012) 331–358.
- [107] Y.F. Yang, K. Cao, T.Z. Wang, Experimental behavior of CFST stub columns after being exposed to freezing and thawing, *Cold Reg. Sci. Technol.* 89 (2013) 7–21.
- [108] H.C. Niu, W.L. Cao, Full-scale testing of high-strength RACFST columns subjected to axial compression, *Mag. Concr. Res.* 67 (5) (2015) 257–270.
- [109] Y.Y. Lu, N. Li, S. Li, et al., Behavior of steel fiber reinforced concrete-filled steel tube columns under axial compression, *Construct. Build. Mater.* 95 (2015) 74–85.
- [110] W.H. Wang, L.H. Han, W. Li, et al., Behavior of concrete-filled steel tubular stub columns and beams using dune sand as part of fine aggregate, *Construct. Build. Mater.* 51 (2014) 352–363.
- [111] F.Y. Huang, X.M. Yu, B.C. Chen, et al., Study on preloading reduction of ultimate load of circular concrete-filled steel tubular columns, *Thin-Walled Struct.* 98 (2015) 454–464.
- [112] M.L. Romero, C. Ibañez, A. Espinos, et al., Influence of ultra-high strength concrete on circular concrete-filled dual steel columns, *Structures* 9 (2017) 13–20.
- [113] L.S. He, Y.g. Zhao, S.Q. Lin, Experimental study on axially compressed circular CFST columns with improved confinement effect, *J. Constr. Steel Res.* 140 (2018) 74–81.
- [114] L.S. He, S.Q. Lin, H.J. Jiang, Confinement effect of concrete-filled steel tube columns with infill concrete of different strength grades, *Frontiers in Materials* 6 (2019) 1–9.
- [115] M.N. Su, Y.C. Cai, X.R. Chen, et al., Behaviour of concrete-filled cold-formed high strength steel circular stub columns, *Thin-Walled Struct.* 157 (2020) 107078.
- [116] Y.H. Yan, H.J. Liang, Y.Y. Lu, et al., Behaviour of concrete-filled steel-tube columns strengthened with high-strength CFRP textile grid-reinforced high-ductility engineered cementitious composites, *Construct. Build. Mater.* 269 (2021) 121283.
- [117] S. Gao, Z. Peng, L.h. Guo, et al., Compressive behavior of circular concrete-filled steel tubular columns under freeze-thaw cycles, *J. Constr. Steel Res.* 166 (2020) 105934.
- [118] S. Gao, L.H. Guo, S.M. Zhang, et al., Performance degradation of circular thin-walled CFST stub columns in high-latitude offshore region, *Thin-Walled Struct.* 154 (2020) 106906.
- [119] Y. Ye, L.H. Han, T. Sheehan, et al., Concrete-filled bimetallic tubes under axial compression: experimental investigation, *Thin-Walled Struct.* 108 (2016) 321–332.
- [120] J.M. Tang, C. Huang, Experimental study on axial compression behavior of high strength concrete-filled steel tubular stub columns, *Ind. Constr.* (2008) 1650–1655.
- [121] W.P. Gu, S.H. Cai, W.L. Feng, Research on the behavior and loading capacity of slender steel tubular columns filled with high-strength concrete, *Build. Sci.* (3) (1991) 3–8.
- [122] W.P. Gu, S.H. Cai, Behavior and ultimate strength of steel tubes filled with high-strength concrete, *Build. Sci.* (1) (1991) 23–27.
- [123] L.H. Han, G.H. Yao, Behaviour of concrete-filled hollow structural steel (HSS) columns with pre-load on the steel tubes, *J. Constr. Steel Res.* 59 (12) (2003) 1455–1475.
- [124] M.S. Guan, C.Q. Wei, Y. Wang, et al., Experimental investigation of axial loaded circular steel tube short columns filled with manufactured sand concrete, *Eng. Struct.* 221 (2020) 111033.
- [125] B.C. Chen, F.Y. Huang, Experimental research on influence of loading methods to behavior of concrete filled steel tubular stub columns under axial loads, *J. China Railw. Soc.* 31 (3) (2009) 82–88.
- [126] L.J. Zhang, Research on Slenderness Ratio of Steel Tube Confined Concrete Short Columns and Medium Long Columns, Inner Mongolia University of Science and Technology, Baotou, 2017 (in Chinese).
- [127] S.T. Zhong, R.Q. He, Study on bearing capacity of concrete filled steel tubular long columns under axial compression, *Journal of Harbin Institute of Architectural Engineering* 1 (1983) 1–13 (in Chinese).
- [128] P.F. Li, T. Zhang, C.Z. Wang, Behavior of concrete-filled steel tube columns subjected to axial compression, *Adv. Mater. Sci. Eng.* 2018 (2018) 4059675.
- [129] B.C. Chen, L.Y. Wang, Z.J. Ou, et al., Experimental study of stress-strain relation of eccentrically-loaded concrete-filled steel tubular columns, *Eng. Mech.* 20 (6) (2003) 154–159.
- [130] M. Johansson, K. Gylltoft, Mechanical behavior of circular steel-concrete composite stub columns, *J. Struct. Eng.* 128 (8) (2002) 1073–1081.
- [131] S.R. Gopal, P.D. Manoharan, Tests on fiber reinforced concrete filled steel tubular columns, *Steel Compos. Struct.* 4 (1) (2004) 37–48.
- [132] Y.J. Chen, Y. Li, W.M. Yan, et al., Bearing capacity test of large size concrete filled steel tubular column, *China J. Highw. Transp.* 24 (4) (2011) 33–38.
- [133] H.L. Wu, Y.F. Wang, Study on size effect of concrete filled steel tubular columns, *J. Harbin Inst. Technol.* 39 (S2) (2007) 22–25 (in Chinese).
- [134] W.L. Jin, X. Zhang, J. Chen, Compressive tests of thin-walled circle concrete-filled steel tubes, *Concrete* (1) (2010) 7–9.
- [135] Z.W. Yu, F.X. Ding, S. Lin, Researches on mechanical behavior of high-performance concrete filled tubular steel stub columns after high temperature, *J. China Railw. Soc.* 25 (4) (2003) 71–79.
- [136] S. Gao, Z. Peng, L.h. Guo, Experimental study on axial performance of concrete-filled steel tubular stub column under salt spray corrosion, *J. Build. Struct.* 40 (S1) (2019) 214–219.
- [137] X.S. Shen, X.Y. Zhang, Y. Fang, et al., Experimental research on axial compression behavior of circular CFST short columns after freeze-thaw cycles, *J. Build. Struct.* 40 (5) (2019) 105–114.
- [138] Z.Y. Lin, Y.H. Wu, Z.Y. Shen, Research on behavior of RPC filled circular steel tube column subjected to axial compression, *J. Build. Struct.* 26 (4) (2005) 52–57.

- [139] Z.Y. Lin, J. Zhang, Y.H. Wu, et al., Experimental investigation on behavior of RPC filled steel stub-column, Fujian Architecture and Construction (3) (2003) 28–30 (in Chinese).
- [140] H. Luo, Research on Behavior of Reactive Powder Concrete-Filled Circular Steel Tube Stub Columns under Axial Compression, Beijing Jiaotong University, Beijing, 2011 (in Chinese).
- [141] G.J. Yang, Research on Behavior and Ultimate Bearing Capacity of Reactive Powder Concrete-Filled Steel Tube Columns under Axial Compression, Beijing Jiaotong University, Beijing, 2013 (in Chinese).
- [142] J.W. Feng, Study on Mechanical Behavior of Reactive Powder Concrete Filled Steel Tubular Columns, Tsinghua University, Beijing, 2008 (in Chinese).
- [143] L.Y. Yao, Researchers on Behavior of Eccentrically Loaded Stub Column and Axially Compressed Slender Column with RPC-Filled Circular Steel Tube, Fuzhou University, Fuzhou, 2004 (in Chinese).
- [144] M. Karmazinová, Buckling Resistance of Concrete-Filled Steel Circular Tube Columns Composed of High-Strength Materials, 2015. London.
- [145] Y.B. Kwon, S.J. Seo, D.W. Kang, Prediction of the squash loads of concrete-filled tubular section columns with local buckling, Thin-Walled Struct. 49 (2011) 85–93.
- [146] J.Y. Zhu, T.M. Chan, Experimental investigation on octagonal concrete filled steel stub columns under uniaxial compression, J. Constr. Steel Res. 147 (2018) 457–467.
- [147] S.Q. Lin, Y.G. Zhao, L.S. He, Stress paths of confined concrete in axially loaded circular concrete-filled steel tube stub columns, Eng. Struct. 173 (2018) 1019–1028.
- [148] A.L. Hoang, E. Fehling, A review and analysis of circular UHPC filled steel tube columns under axial loading, Struct. Eng. Mech. 61 (2) (2017) 417–430.
- [149] T. Tao, D.C. Zhang, B. Sun, et al., Behavior of self-compacting concrete-filled Q460 high-strength steel tubular short columns under axial compression, J. Civ. Eng. Manag. 33 (5) (2016) 54–58.
- [150] Y.Y. Lu, S. Li, S. Li, et al., Study on property of concentrically compressed concrete filled circular FRP-steel tube stub columns, J. China Railw. Soc. 38 (4) (2016) 105–111.
- [151] J.B. Yan, T. Wang, X. Dong, Compressive behaviours of circular concrete-filled steel tubes exposed to low-temperature environment, Construct. Build. Mater. 245 (2020) 118460.
- [152] G. Song, Study on Restraint Effect and Axial Compression Behavior of Large Diameter Concrete Filled Steel Tube, Xihua University, Chengdu, 2020 (in Chinese).
- [153] X.B. Long, Experimental and Numerical Investigations on Concrete-Filled Steel Tubular Stub Columns under Axial Compression, Hunan University, Changsha, 2014 (in Chinese).
- [154] Z.H. Xu, Experimental Study and Analysis of RPC-Filled Steel Tube under Axial Compression and Push Out Test, Hunan University, Changsha, 2016 (in Chinese).
- [155] S.T. Zhong, Y.C. Wang, Discussion on the calculation of working performance and bearing capacity of concrete-filled steel tubular members under axial compression, Journal of Harbin Institute of Architectural Engineering 1 (1978) 1–33 (in Chinese).
- [156] G.Z. Tang, B.Q. Zhao, H.X. Zhu, et al., Study on the fundamental structural behavior of concrete filled steel tubular columns, J. Build. Struct. 3 (1) (1982) 13–31.
- [157] S.H. Cai, Z.S. Jiao, Behavior and ultimate strength of short concrete-filled steel tubular columns, J. Build. Struct. (6) (1984) 13–29.
- [158] S.H. Cai, X.T. Di, Behaviour and ultimate strength of concrete-filled steel tubular columns under eccentric loading, J. Build. Struct. (4) (1985) 33–43.
- [159] S.H. Cai, W.L. Gu, Behaviour and ultimate strength of long concrete-filled steel tubular columns, J. Build. Struct. 1 (1985) 32–40.
- [160] W.P. Gu, S.H. Cai, W.L. Feng, Behavior and bearing capacity of eccentrically loaded steel tubular columns filled with high-strength concrete, Build. Sci. (3) (1993) 8–12.
- [161] K.F. Tan, X.C. Pu, S.H. Cai, Study on the mechanical properties of steel extra-high strength concrete encased in steel tubes, J. Build. Struct. 20 (1) (1999) 10–15.
- [162] T. Yamamoto, J. Kawaguchi, S. Morino, et al., Scale Effect on Compression Behavior of Concrete-Filled Steel Tube Short Columns, Research Reports of the Faculty of Engineering, Mie University, 2000, pp. 27–44.
- [163] G. Giakoumelis, D. Lam, Axial capacity of circular concrete-filled tube columns, J. Constr. Steel Res. 60 (2004) 1049–1068.
- [164] L.H. Han, G.H. Yao, Experimental behaviour of thin-walled hollow structural steel (HSS) columns filled with self-consolidating concrete (SCC), Thin-Walled Struct. 42 (2004) 1357–1377.
- [165] C.Y. Lin, Axial Capacity of Concrete Infilled Cold-Formed Steel Columns, International Specialty Conference on Cold-Formed Steel Structures, Missouri, USA, 1988, pp. 443–457.
- [166] Q. Yu, Z. Tao, Y.X. Wu, Experimental behaviour of high performance concrete-filled steel tubular columns, Steel Construction 46 (2008) 362–370.
- [167] S.H. Lee, B. Uy, S.H. Kim, et al., Behavior of high-strength circular concrete-filled steel tubular (CFST) column under eccentric loading, J. Constr. Steel Res. 67 (2011) 1–13.
- [168] M. Dundu, Compressive strength of circular concrete filled steel tube columns, Thin-Walled Struct. 56 (2012) 62–70.
- [169] Y.F. Yang, L.H. Han, Concrete filled steel tube (CFST) columns subjected to concentrically partial compression, Thin-Walled Struct. 50 (2012) 147–156.
- [170] X. Chang, L. Fu, H.B. Zhao, et al., Behaviors of axially loaded circular concrete-filled steel tube (CFT) stub columns with notch in steel tubes, Thin-Walled Struct. 73 (2013) 273–280.
- [171] J.M. Portolés, E. Serra, M.L. Romero, Influence of ultra-high strength infill in slender concrete-filled steel tubular columns, J. Constr. Steel Res. 86 (2013) 107–114.
- [172] K. Pearson, Note on regression and inheritance in the case of two parents, Proc. Roy. Soc. Lond. 58 (347–352) (1895) 240–242.
- [173] V.L. Tran, S.E. Kim, D.K. Thai, A new empirical formula for prediction of the axial compression capacity of CCFT columns, Steel Compos. Struct. 33 (2) (2019) 181–194.
- [174] MATLAB, MATLAB R2020b, The MathWorks, Natick, Massachusetts, USA, 2020.
- [175] W.S. McCulloch, W. Pitts, A logical calculus of the ideas immanent in nervous activity, Bull. Math. Biophys. 5 (1943) 113–115.
- [176] F. Rosenblatt, The perceptron: a probabilistic model for information storage and organization in the brain, Psychol. Rev. 65 (6) (1958) 386–408.
- [177] B.B. Zha, R.L. Wang, H.L. Sun, et al., A Study of the Design and Parameters Optimization of BP Neural Network Using Improved GEP, 10th International Conference on Computational Intelligence and Security, 2014.
- [178] D.E. Goldberg, Genetic Algorithms in Search, Optimization, and Machine Learning, Addison-Wesley Publishing Company, INC, USA, 1988.
- [179] J. Moody, C.J. Darken, Learning with localized receptive fields, in: Proceedings of the 1988 Connectionist Models Summer School, 1988, pp. 133–143.
- [180] J. Moody, C.J. Darken, Fast learning in networks of locally-tuned processing units, Neural Comput. 1 (1989) 281–294.
- [181] C.E. Rasmussen, C.K.I. Williams, Gaussian Processes for Machine Learning, MIT Press, 2006.
- [182] S. Thai, H.T. Thai, B. Uy, et al., Concrete-filled steel tubular columns: test database, design and calibration, J. Constr. Steel Res. 157 (2019) 161–181.